1. THE FORMATION OF PLANETESIMALS

2. TIDAL FRICTION AND GENERALIZED CASSINI'S LAWS IN THE SOLAR SYSTEM

Thesis by

William Roger Ward

In Partial Fulfillment of the Requirements

For the Degree of

Doctor of Philosophy

California Institute of Technology

Pasadena, California

1973

(Submitted November 21, 1972)

To my wife, Sandy

ACKNOWLEDGMENTS

I would like to thank my thesis advisor, Professor Peter Goldreich, for giving generously of his time and experience during the course of this investigation. Indeed, the first part of this thesis reports the results of a research project upon which we have collaborated for the better part of a year. Professor Goldreich also supplied several valuable suggestions concerning the exposition of the second part of this thesis.

I also thank Professor Duane O. Muhleman for several encouraging discussions, as well as for reading the preliminary drafts of this thesis and indicating numerous ways to improve the presentation of Part 2.

Dr. Olav L. Hansen was of considerable help in the computer portion of this research. I am also indebted to Mrs. Kay Campbell who spent many extra hours preparing the manuscript.

To my parents, Mr. and Mrs. John K. Ward, I am tremendously grateful for their unfailing support throughout my education.

Finally, I wish most deeply to thank my wife, Sandy, whose understanding and patience through these years has made the completion of this work possible. In a very true sense of the word, this is our thesis.

The author was supported by a National Defense Education Act Title IV Fellowship during much of the period that this research was carried out. A portion of the research costs were also furnished by NASA Grant NGL 05-002-003.

ABSTRACT

In Part 1, four stages in the accretion of planetesimals are described. The initial stage is the condensation of dust particles from the gaseous solar nebula as it cools. These dust particles settle into a thin disk which is gravitationally unstable. A first generation of planetesimals, whose radii range up to $\sim 10^{-1}$ kilometer, form from the dust disk by direct gravitational collapse to solid densities on a time scale of order one year. The resulting disk, composed of first generation planetesimals, is still gravitationally unstable and the planetesimals are grouped into clusters containing approximately 10^4 members. The contraction of these clusters is controlled by the rate at which gas drag damps their internal rotational and random kinetic energies. On a time scale of a few thousand years, the clusters contract to form a second generation of planetesimals having radii of the order of a few kilometers. Further coalescence of planetesimals proceeds by collisions which seem capable of producing objects with a growth rate of ~ 15 cm. yr^{-1} at one A.U. The final stage of accretion during which planet-sized objects form is not considered here.

In Part 2 of this thesis, an investigation of a dynamical problem which has considerable application to the solar system is undertaken. The evolution of the obliquity of an object is determined when under the influence of three phenomena: (1) the precession of the object's orbit plane, (2) the precession of the object's spin axis, and (3) tidal friction. In the absence of tidal friction, it is concluded that if the period for precession of the spin axis is much shorter than the orbit precession period, the obliquity of the object will remain very nearly constant in spite of the movement of the orbit normal. It is further concluded, that since the obliquity is not changed by

the motion of the orbit plane, the decay of the obliquity towards zero by tidal friction is not significantly altered by this motion. These results are applied to Mercury, Venus, Iapetus, Triton, as well as the equatorial satellites of Mars, Jupiter, Saturn, and Uranus. The final spin states of these objects satisfy a generalization of Cassini's laws for the moon.

TABLE OF CONTENTS

	Page
PART 1. THE FORMATION OF PLANETESIMALS	1
I Introduction	2
II The Particulate Disk	6
a Formation	6
b Gas Drag and Orbit Decay	8
III Fragmentation and Collapse	13
a Stability	13
b Fragmentation	16
c Further Growth	19
d Survival Time	20
IV Discussion	22
References	24
PART 2. TIDAL FRICTION AND GENERALIZED CASSINI'S LAWS IN THE SOLAR SYSTEM	25
I Introduction	26
II Equations	31
a Orbit Precession	31
b Spin Precession	37
III Geometry	44
a Prograde Rotation	47
i Mercury	49
ii Moon	50
iii Triton	50
iv Iapetus	51

TABLE OF CONTENTS

		Page
III	Geometry (Continued)	
	v Equatorial Satellites	52
	b Retrograde Rotation	55
IV	Tidal Friction and Generalized Cassini's Laws	57
	a Frequency Dependent Q	58
	b Constant Q	62
	c Physical Interpretation	63
V	Obliquity of Mercury	68
VI	Obliquity of Venus	84
VII	Conclusion	87
	Appendix	89
	References	93

FIGURES

Number		Page
1	Composite Schematic of Spin Precession and Orbit Plane Precession of a Secondary	33
2	The Rotating Coordinate System	40
3	The Auxiliary Vector, $\hat{\xi}$	46
4	Tidal Decay of Spin Vector Toward $\hat{\xi}$	66
5	Decay of Mercury's Spin for Different Initial Obliquities	72
6	Decay of Mercury's Spin for Different Orbital Eccentricities	75
7	Location of Principal Axes of an Object in the 3/2 Resonance State with a Non-zero Obliquity	78

TABLE OF CONTENTS

Number		Page
	FIGURES (Continued)	
8	Decay of the Obliquity of an Object in the 3/2 Resonance State	82
	TABLES	
1	Inclination of Planetary Orbits	27
2	Spin Precession Periods of the Planets	53
3	Spin Precession Periods for Hydrostatically Flattened Satellites	54

PART 1. THE FORMATION OF PLANETESIMALS

I. INTRODUCTION

This paper reports on an investigation of the significance of gravitational instabilities in the primordial solar nebula to the planetary formation process. Of course, this subject is by no means a new one. Kuiper (1951) suggested that fragmentation of the nebula into protoplanets occurred when compression of the disk in the vertical direction due to cooling drove the density above the local Roche limit. However, he did not determine the scale of the instabilities but merely assumed that it was comparable to the planetary separations. An attempt to establish this scale was made by Urey (1966, 1972). Urey applied the dispersion relation for an infinite uniformly rotating gas to the solar nebula. This dispersion relation reads (Chandrasekhar 1955)

$$\omega^2 = k^2c^2 + 4\Omega^2 - 4\pi G\rho, \tag{1}$$

where ρ is the unperturbed gas density, c is the sound speed, Ω is the angular velocity, G is the gravitational constant, ω is the frequency of the disturbance and $k = 2\pi/\lambda$ is its wave number. From the above dispersion relation, we see that a range of unstable wavelengths exists if $\pi G\rho > \Omega^2$. The minimum unstable wavelength is

$$\lambda_{min} = \pi c/(\pi G\rho - \Omega^2)^{1/2}. \tag{2}$$

Urey assumed that $\pi G\rho$ was slightly greater than Ω^2. He then deduced that lunar sized objects formed as the products of the collapse of regions of initial sizes λ_{min}. One puzzling feature of Urey's work is his choice of λ_{min} as the dominant instability scale since Chandrasekhar's dispersion relation shows that longer wavelength perturbations grow faster.

These attempts to attribute the planetary formation process to gravitational instabilities of the entire gaseous nebula encounter an insurmountable obstacle. The density required for instability is so great that either the temperature of the nebula must have been unacceptably low or else its mass must have greatly exceeded the value needed to account for the present combined masses of the planets. A brief discussion of this point is given in § IIIa.

Our contribution is to outline the process by which dust particles accreted to form gravitationally active objects. We shall present a compelling argument that, indeed, gravitational instabilities accounted for the growth of objects up to several kilometers in radius. The crucial difference between our investigation and earlier analyses is that these instabilities are found to develop, not in the gaseous solar nebula, but in the thin disk of particulate matter that forms in the central plane during the condensation phase. While our work was in progress, two papers dealing with this problem have appeared. Lyttleton (1972) pointed out that a thinning dust disk would eventually become more dense than the Roche limit. But he made no attempt to ascertain the masses of the unstable regions. Polyachenko and Fridman (1972) presented an analysis of the fragmentation of a dust disk similar to that contained in § IIIa of this paper. They solved for the density of a dust disk which would have been unstable on the scale of the present planetary separations. Not surprising, they found that the required mass of solid material was orders of magnitude greater than that present in the planets. On the other hand, we use the known masses of the planets to estimate the

surface density of the preplanetary dust disk and then solve for the scale of the initial instabilities.

In section §II, formation of the thin disk of condensed particles and its further evolution through gas drag will be described. The fragmentation of the disk is treated in §III and the formation time and masses of the resulting planetesimals are calculated. It should be emphasized at the outset that at several stages of this investigation assumptions are introduced for which alternate possibilities are also quite plausible. In order to keep our exposition as lucid as possible, we shall follow one particular line of reasoning through to the end. Then in the concluding section, we shall explore the modifications which the competing assumptions would have introduced.

In order to avoid repetitious references to the numerical values of the physical parameters appropriate to the primordial solar nebula, we list here our adopted values for the vicinity of the Earth's orbit. These values will be applied in the text to all numerical calculations without further reference. The distance from the sun is $a = 1.5 \times 10^{13}$ cm and the Keplerian mean motion is $\Omega = 2 \times 10^{-7}\ s^{-1}$. The surface density of condensed matter implied by the masses of the terrestrial planets is $\sigma_p \sim 7.5$ gm cm^{-2}, which represents a mass fraction $\alpha \sim 5 \times 10^{-3}$ of the entire gaseous preplanetary disk whose surface density $\sigma_g \sim 1.5 \times 10^{3}$ gm cm^{-2}. We shall use a value of $c = 7.6 \times 10^{3}\ T^{1/2}$ cm s^{-1} for the speed of sound at temperature T. This expression is applicable to a gas composed of hydrogen molecules. Where a specific value for T is required, we shall use $T = 700^{\circ}$ K. The half-thickness of the gas disk is $D \sim c/\Omega \sim 10^{12}$ cm, which implies a mean gas density of $\rho_g \sim 7.5 \times 10^{-10}$ gm cm^{-3}. The mean free path in the gas is $\ell_g \sim 10$ cm, which together

with the value for c, yields $\nu \sim 2 \times 10^6$ cm^2 s^{-1} for the kinematic viscosity. In the discussion of the chemical condensation of dust particles we shall use numerical values appropriate for iron. These are $\alpha(\mathrm{Fe}) = 1.5 \times 10^{-3}$ and $\rho_p(\mathrm{Fe}) = 7.9$ gm cm^{-3}. Elsewhere, we shall assume $\rho_p \sim 3$ gm cm^{-3} as appropriate for the mean uncompressed density of the terrestrial planets.

II. THE PARTICULATE DISK

a) Formation

An attractive hypothesis for the initial stage of planetary accretion has emerged from recent studies of the chemical condensation sequence of the cooling preplanetary gas. As the primordial solar nebula cools, the vapor pressure of a constituent rapidly decreases and eventually falls below its partial pressure. Presumably, at this stage the condensation of small particles ensues. The importance of this process has long been recognized but has only recently begun to be investigated in detail (Lord 1965; Larimer 1967; Larimer and Anders 1970; Lewis 1972). From the present composition of the terrestrial planets, it appears that the principal condensates in the inner solar system are iron, nickel, and iron and magnesium silicates (Larimer 1967). In the outer nebula the temperatures are lower and the bulk of the condensate is made up of water and water-ammonia ices (Lewis 1972).

Once nucleation occurs, a particle continues to grow by collecting material still in vapor phase. Its growth rate is given by (Hoyle 1946)

$$\frac{dr}{dt} = \alpha \, v_T \frac{\rho_g}{\rho_p} , \qquad (3)$$

where r is the particle's radius and v_T is the thermal velocity of the constituent molecules which are still in the vapor phase. Numerically, the growth rate is on the order of centimeters per year for the more abundant minerals.

Once nucleated, a particle begins to settle through the gas toward the equatorial plane where it can no longer collect material from the vapor phase.

This sets a definite upper limit on the size a particle can obtain. In order to calculate this limiting size, we must estimate the rate at which a particle descends to the central plane. The differential velocity between a descending particle and the local gas is set by the balance between the vertical component of solar gravity and the gas drag force. For the small particles with which we are concerned, the mean free path in the gas is long compared to the particle radius and the drag force is given by

$$F_D \sim \pi r^2 \rho_g \, c \, v_z \tag{4}$$

where v_z is the vertical velocity of the particle. Setting this expression equal to the vertical force of solar gravity, we find

$$v_z \sim \Omega^2 \frac{\rho_p z}{\rho_g c} r \ . \tag{5}$$

Since the half-thickness of the gas disk is approximately c/Ω, the characteristic descent time may be expressed in terms of the surface density of the gas disk as

$$\tau_z \sim \frac{1}{\Omega} \frac{\sigma_g}{\rho_p} \frac{1}{r} \ . \tag{6}$$

From equations (3) and (6), it follows that the maximum radius, R, to which a particle can grow before reaching the central plane is

$$R \sim \frac{\alpha^{1/2} \sigma_g}{\mu^{1/4} \rho_p} \ , \tag{7}$$

where μ is the molecular weight of the condensing molecules. When applied to the condensation of iron in the terrestrial region, equations (6) and (7) yield $\tau_z \sim 10$ yr and $R \sim 3$ cm.

It is obvious that the unknown number of nucleation sites is the principal uncertainty bearing on the size of the particles which settle into the central dust disk. If the number of these sites is so large that the vapor phase is significantly depleted on time scales short compared to the particle descent time, the final particle sizes will be much smaller than R given by equation (7). Because we have no handle on the actual number of nucleation sites, we shall express all future results in terms of the unknown particle radius $r \lesssim R$.

b) Gas Drag and Orbital Decay

In addition to a vertical pressure gradient, there undoubtedly exists a radial pressure gradient in the gaseous solar nebula. This affects the orbital velocity of the gas since the centripetal acceleration is produced by the difference between the inward gravitational attraction of the sun and the outward force of the pressure gradient. Thus,

$$a\Omega_g^2 = \frac{GM_\odot}{a^2} + \frac{1}{\rho_g}\frac{dp_g}{da} \quad , \tag{8}$$

where Ω_g is the orbital angular velocity of the gas, $M_\odot$ is the mass of the sun and p_g is the gas pressure. If we make the approximation $dp_g/da \sim -c^2\rho_g/a$, then we obtain

$$\Omega_g \sim \Omega - \frac{c^2}{2\Omega a^2} \tag{9}$$

to lowest order in $(c/\Omega a)^2 \ll 1$. Here Ω is the local Keplerian velocity.

The pressure gradient has little effect on the condensed particles since their densities are many orders of magnitude higher than the gas density. However, the particles do interact with the gas through gas drag. A straight-forward calculation for the rate at which a particle spirals toward the sun yields

$$\frac{\dot{a}}{a} \sim - \frac{2\chi\Omega}{(4\chi^2 + \Omega^2)} (\Omega - \Omega_g) , \tag{10}$$

where

$$\chi = \frac{3}{4} \frac{\rho_g}{\rho_p} \frac{c}{r} \quad . \tag{11}$$

From equations (9), (10) and (11) it follows that the characteristic orbital decay time, $\tau_a = a/\dot{a}$, is given by

$$\tau_a \sim \frac{3\rho_g a^2}{\rho_p c r} \quad , \tag{12}$$

where we have used the fact that

$$\frac{\chi}{\Omega} = \frac{3}{4} \frac{\sigma_g}{\rho_p r} > \frac{3}{4} \frac{\sigma_g}{\rho_p R} \sim \frac{3}{4} \frac{\mu^{1/4}}{\alpha^{1/2}} >> 1 \ . \tag{13}$$

The fractional decay that a particle's orbital radius suffers during the particle's descent to the central plane is

$$\frac{\Delta a}{a} \sim \frac{\tau_z}{\tau_a} \sim \frac{1}{3} \left(\frac{c}{a\Omega} \right)^2 \sim 10^{-3} \ . \tag{14}$$

The characteristic orbital decay time given by equation (12) is

$$\tau_a \sim \frac{2 \times 10^4}{r} \text{ yr} \tag{15}$$

in the terrestrial region ($a \sim 1$ AU), where r is to be expressed in centimeters. The estimate given above for τ_a is not applicable to particles in the dust disk unless gas molecules are able to pass freely through the disk. The ratio of the mean free path, ℓ_p, to the thickness of the disk, d, is approximately

$$\frac{\ell_p}{d} \sim \frac{4\rho_p r}{3\sigma_p} \sim 0.53r \ . \tag{16}$$

From equation (16), we see that if a substantial fraction of the particles in the disk have radii in the sub-centimeter range, then $\ell_p/d < 1$. In this case, the gas drag is exerted on the surface of the dust disk. A short calculation of this boundary layer drag is outlined below.

The drag force per unit area on the surface of the disk is given by

$$S = \rho_g \nu \frac{dv_g}{dz} \ , \tag{17}$$

where ν is the kinematic viscosity in the gas. If the boundary layer flow were laminar, the velocity gradient would be confined to an Ekman boundary layer of thickness

$$\delta \sim \sqrt{\nu/\Omega} \ . \tag{18}$$

From the standard parameters we have adopted, it follows that $\delta \sim 3 \times 10^6$ cm, is much smaller than the half-thickness of the gaseous disk, $D \sim 10^{12}$ cm. The tangential stress on the dust disk would be

$$S \sim \frac{\rho_g \nu a(\Omega_g - \Omega)}{\delta} \sim -\frac{1}{2}\left(\frac{\nu}{\Omega a^2}\right)^{1/2} \rho_g c^2 . \qquad (19)$$

However, it seems quite likely that the boundary layer flow is turbulent. The Reynolds number in the Ekman layer, if the flow is assumed to be laminar, is

$$Re \sim \frac{a(\Omega - \Omega_g)\delta}{\nu} \sim \frac{c^2}{2\nu^{1/2}\Omega^{3/2}a} \sim 10^4 . \qquad (20)$$

Furthermore, gravitational stratification appears to be too weak to stabilize the boundary layer flow since the Richardson number (e.g., Chandrasekhar 1961) is

$$Ri \sim -\frac{g_z d\rho/dz}{\rho(dv_g/dz)^2} \sim \frac{8\pi G\sigma_p \nu}{c^3}\left(\frac{\Omega a}{c}\right)^2 \sim 10^{-12} , \qquad (21)$$

much smaller than the critical value of 1/4.

The tangential stress due to a turbulent boundary layer is given by equation (17) but with ν replaced by the turbulent viscosity

$$\nu' \sim \frac{\Delta v_g \delta'}{Re^*} . \qquad (22)$$

Here $\Delta v_g \sim (\Omega - \Omega_g)a$ is the velocity jump across the boundary layer, δ' is the boundary layer thickness, and Re* is the critical value of the Reynolds number above which the flow becomes fully turbulent. Since $dv_g/dz \sim \Delta v_g/\delta'$, the turbulent stress on the disk is simply

$$S \sim \frac{\rho_g \Delta v_g^2}{Re^*} . \qquad (23)$$

From experimental data it is known that $Re^* \sim 5 \times 10^2$ (Jeffreys 1959). The thickness of the turbulent boundary layer is

$$\delta' \sim \frac{\Delta v_g}{\Omega Re^*} \sim \frac{1}{2}\left(\frac{c}{\Omega a}\right)^2 \frac{a}{Re^*} \sim 7 \times 10^7 \text{ cm.} \qquad (24)$$

The lifetime of the dust disk against orbital decay turns out to be

$$\tau_a \sim 2\alpha \left(\frac{\Omega a}{c}\right)^2 \frac{c}{(\nu\Omega)^{1/2}} \frac{1}{\Omega} \sim 1 \times 10^5 \text{ yr} \quad , \qquad (25)$$

if the boundary layer flow is laminar and

$$\tau_a \sim 4Re^*\alpha \left(\frac{\Omega a}{c}\right)^3 \frac{1}{\Omega} \sim 5 \times 10^3 \text{ yr} \quad , \qquad (26)$$

in the more likely case that it is turbulent. From equations (15) and (26), it appears that the time available to initiate the next stage of the accretion process (following the condensation of small particles from the vapor phase) is about 10^3 years.

III. FRAGMENTATION AND COLLAPSE

a) Stability

Extensive calculations of the gravitational stability of rotating disks have been carried out in an effort to explain the spiral structure of galaxies (Toomre 1964; Goldreich and Lynden-Bell 1965 a, b). We shall make use of the dispersion relation for local axisymmetric perturbations (i.e., for wavelengths $\lambda \ll a$) which reads

$$\omega^2 = k^2 c^2 + \kappa^2 - 2\pi G \sigma k \quad , \tag{27}$$

where $\kappa^2 = 2\Omega[\Omega + d(r\Omega)/dr]$ and c is the sound speed. The important features to note are that pressure stabilizes short disturbances and rotation stabilizes long ones. If the surface density σ is high enough, there is a range of intermediate wavelengths which are unstable. For a given c and κ, the critical value of σ above which the disk is unstable is given by

$$\sigma^* = \frac{\kappa c}{\pi G} \quad . \tag{28}$$

This criterion is not rigorously applicable to the gaseous solar nebula since it is derived for a thin disk. Nevertheless, it does provide a good estimate of the surface density required for instability. If we substitute in equation (28) $\kappa = \Omega$, which is the appropriate expression for Keplerian motion, the critical gas surface density is

$$\sigma_g^* = 7.6 \times 10^3 \, T^{1/2} \text{ gm cm}^{-2}. \tag{29}$$

Since the value of σ_g we obtain by augmenting the terrestrial planets up to solar composition is only 1.5×10^3 gm cm^{-2}, equation (29) implies that the gaseous solar nebula is stable unless $T < 0.04^\circ K$. Actually, equation (29) gives an underestimate of the critical surface density for a gas disk of finite thickness by a factor of order 3. This is a consequence of basing the derivation of σ^* on a thin disk model which overemphasizes the effects of the disk's self-gravitation for disturbances which are not much longer than its thickness. The low temperature required by equation (29) is the primary reason for rejecting planetary formation theories which are based on the gravitational instability of the gaseous solar nebula.

We now proceed to apply the dispersion relation given by equation (27) to the stability of the dust disk which forms in the equatorial plane of the solar nebula.

The interpretation of c in this context requires some discussion. The use of a sound speed, c, to model the effect of the random kinetic energy of dust particles is not entirely justified because collisions between particles are inelastic. The time interval between collision, τ, is given by $\tau \sim \ell_p/c$, where ℓ_p is the particle mean free path. The mean free path is $\ell_p \sim 4r\rho_p d/3\sigma_p$, where d is the thickness of the dust layer. The thickness is in turn a function of the dispersion velocity since it is just twice the height to which a typical particle can rise above the central plane. Thus,

$$d \sim c^2/2\pi G\sigma_p \ . \tag{30}$$

Note that the disk's self-gravity has been used in deriving equation (30) and not the vertical component of the sun's gravity. This is because inside the

disk, the gravitational acceleration due to the disk, $2\pi G\sigma_p z/d$, exceeds the vertical component of the solar gravitational acceleration, $GM_\odot z/a^3 = \Omega^2 z$, for disks which are cold enough to be unstable. If at each collision a fraction β of the impacting particles' kinetic energy is dissipated as heat, the velocity dispersion will damp on a time scale of order

$$\tau_{damping} \sim \frac{2c\rho_p r}{3\pi G\sigma_p^2 \beta} \sim 2 \times 10^5 \frac{cr}{\beta} \text{ s} , \tag{31}$$

where c and r are to be expressed in cgs units. From equation (28), it follows that $c < \pi G\sigma_p/\kappa$ in unstable disks. With our standard parameters, this implies $c < 8$ cm s^{-1} and hence, $\tau_{damping} < 1.6 \times 10^6 r/\beta$ seconds. Thus for most applications we can safely set $c = 0$. The principal exceptions arise in cases of collapse on time scales shorter than $\tau_{damping}$.

In the absence of random motions ($c = 0$), the dust disk is unstable to all axisymmetric perturbations of wavelength shorter than the critical wavelength

$$\lambda_c = 4\pi^2 G\sigma_p/\Omega^2 . \tag{32}$$

For uniformly rotating disks, the stability criterion for non-axisymmetric perturbations is the same as that for the axisymmetric ones. The situation is more complicated for differentially rotating disks. The shear associated with the differential rotation converts an arbitrary non-axisymmetric disturbance into an approximately axisymmetric one in a time of order a few rotation periods. Fortunately, as equation (27) shows, the growth time for perturbations having wavelengths shorter than λ_c is less than an orbital period. (Actually, equation (27) only shows this for axisymmetric

disturbances, but the same result also holds for more general perturbations.) Thus, for perturbations which are somewhat smaller than λ_c, we can forget the distinction between axisymmetric and more general perturbations and just use equation (27) to get an estimate of the exponential growth rate. The exact value of $\lambda < \lambda_c$, below which equation (27) may be used for non-axisymmetric perturbations, is not well-defined. It depends upon the magnitude of the initial perturbation which determines how fast growth into the non-linear regime is achieved. We shall express all future results in terms of $\xi\lambda_c$, where ξ is on the order of, but less than, unity.

b) Fragmentation

The largest fragments that form when the unstable disk breaks up have masses of order $m \sim \sigma_p \xi^2 \lambda_c^2$. Numerically, $\lambda_c \sim 5 \times 10^8$cm and $m \sim 2 \times 10^{18} \xi^2$ gm. Note that $\lambda_c \ll a$, so that our application of the dispersion relation given in equation (27) is justified.

Regions containing total masses as large as m cannot collapse unimpeded. As a fragment contracts, its gravitational binding energy, U', increases as $U' \sim U\lambda/\lambda'$. However, as a consequence of the conservation of internal angular momentum, its rotational energy, E_R', increases as $E_R' \sim E_R(\lambda/\lambda')^2$. Furthermore, if the contraction time scale is shorter than the damping time for random motions, the random kinetic energy of the particles, T', increases as $T' \sim T(\lambda/\lambda')^2$. If the release of gravitational binding energy exceeds the demands of the rising rotational and internal kinetic energies, the excess energy will appear in the form of a bulk contraction velocity. On the other hand, if during the collapse, the required rate of increase of rotational and

random kinetic energies cannot be met by the release of gravitational potential energy, the contraction velocity will decay and re-expansion will ensue. In this latter case, the dimension of the fragment will eventually begin to oscillate about an equilibrium size which is determined by

$$\frac{d}{d\lambda'}(E_R' + T' - U') = 0, \tag{33}$$

or, in differentiated form, by

$$2E_R' + 2T' - U' = 0 \ . \tag{34}$$

The condition for marginal stability ($\omega^2 = 0$) given by the dispersion relation (eq. [27]) is of this form. In terms of the wavelength λ, it yields

$$\lambda^2\Omega^2 + 4\pi^2 c^2 - 4\pi^2 G\sigma_p \lambda = 0 \tag{35}$$

for the marginally stable mode. We may identify each of the three terms in equation (34) with the corresponding term in equation (35). Consider next an unstable linear perturbation of the dust disk (i.e. one for which $\omega^2 < 0$) of wavelength λ. In the absence of interactions with other contracting fragments, this perturbed region would initially collapse and then oscillate about an equilibrium size λ' given by

$$(\lambda^2\Omega^2 + 4\pi^2 c^2)\left(\frac{\lambda}{\lambda'}\right)^2 - 4\pi^2 G\sigma_p \lambda \left(\frac{\lambda}{\lambda'}\right) = 0 \tag{36}$$

or

$$\lambda' = \frac{\lambda^2\Omega^2 + 4\pi^2 c^2}{4\pi^2 G\sigma_p} \ . \tag{37}$$

As written, equations (36) and (37) do not include the effects of damping on the random motions of the particles. However, it seems likely that damping is always fast enough to make the random motions unimportant to the collapse dynamics. To appreciate this, note that the damping time as given in equation (31) depends inversely on σ_p^2 and thus decreases as $(\lambda'/\lambda)^4$ as the collapse proceeds. The characteristic time scale for collapse is never shorter than $\sim(\lambda'/G\sigma_p)^{1/2}$ and thus, decreases more slowly as $(\lambda'/\lambda)^{3/2}$. From the numerical estimate of the damping time given by equation (31), it appears that the damping of the random kinetic energy is sufficiently rapid to render pressure unimportant in the initial stages of the contraction. The preceeding argument then implies that the effects of pressure remain small for all later stages of collapse.

Fragments collapse directly to form solid bodies provided that their equilibrium contraction corresponds to spatial densities at least as great as that of the solid material. The condition on the equilibrium contraction is approximately

$$\frac{\lambda}{\lambda'} \gtrsim \left(\frac{\pi\rho_p\lambda}{6\sigma_p}\right)^{1/3} . \tag{38}$$

If equation (37) is substituted into the above inequality (and the initial random kinetic energy is set to zero) we obtain

$$\lambda^4 \lesssim \frac{384\pi^5 G^3\sigma_p^4}{\Omega^6\rho_p} = 384\pi^5 \left(\frac{\Omega^2}{G\rho_p}\right)\left(\frac{G\sigma_p}{\Omega^2}\right)^4 , \tag{39}$$

or numerically,

$$\lambda \leq 5 \times 10^6 \text{ cm} \quad . \tag{40}$$

The mass and diameter of the solid bodies which form from fragments of initial size λ are $m \leq 2 \times 10^{14}$ gm and $\lambda' \leq 0.5$ km.

c) Further Growth

We have shown how dust particles coalesce into planetesimals with radii of a few tenths of kilometers. Because $\lambda_c/\lambda \sim 10^2$, these first generation planetesimals will be grouped into rotating disk-like associations containing $\sim 10^4 \xi^2$ members. Although each cluster is stable against collapse on the gravitational free-fall time scale, it does contract slowly as gas drag reduces its internal rotational and random kinetic energy. Since the Reynolds number for the gas flow about bodies the size of the planetesimals is large, the drag force arises from the formation of a turbulent wake and is

$$\underset{\sim}{F}_D = C_D \pi r^2 \rho_g |\underset{\sim}{v}_g - \underset{\sim}{v}_p| (\underset{\sim}{v}_g - \underset{\sim}{v}_p) \tag{41}$$

where C_D is the dimensionless drag coefficient typically on the order of a few tenths. The contraction time for the associations is then given by

$$\tau \sim \frac{4}{3C_D} \left(\frac{\rho_p}{\rho_g}\right) \left(\frac{a\Omega}{c}\right) \frac{r}{c} \sim 1.3 \times 10^2 r_4 / C_D \text{ yr} \quad , \tag{42}$$

where r_4 is the radius in units of tenths of kilometers. It is easily shown that the cluster contraction time is comparable to the relaxation time due to binary encounters between planetesimals. Thus, the contraction of a cluster should proceed without a significant loss of members by evaporation. The masses and radii of the second generation of planetesimals range up to

$$m \sim \lambda_c^2 \xi^2 \sigma_p \sim 2 \times 10^{18} \xi^2 \text{ gm} \tag{43}$$

and

$$r \sim 5\,\xi^{2/3} \text{ km} \quad . \tag{44}$$

Beyond this stage it appears unlikely that further growth proceeds by means of collective gravitational instabilities such as we have been describing. The frictional effect of gas drag does destabilize axisymmetric perturbations for wavelengths larger than λ_c. We cannot be certain that the axisymmetric perturbations by themselves are not a significant feature in producing a limited further growth of planetesimals. However, it is possible to prove that they are too slow to be responsible for the accumulation of material over interplanetary distances.

Direct particle-particle collisions are probably the dominant accretion process following the formation of the second generation planetesimals. It seems plausible to expect near encounters between planetesimals to build up a dispersion velocity on the order of the escape velocity from the surface of a typical object $v_e = (2GM/r)^{1/2}$. The corresponding disk thickness is $d \sim v_e/\Omega$. The growth rate produced by direct impacts is simply

$$\frac{dr}{dt} \sim \frac{\Omega \sigma_p}{\rho_p} \sim 15 \text{ cm yr}^{-1} \quad . \tag{45}$$

d) Survival Time

As long as the gaseous solar nebula is present, gas drag will produce a slow inward drift of the planetesimals toward the sun. It is essential that at each stage of accretion, the particle growth time be short compared to the orbital lifetime set by gas drag. We have already verified that this

condition is well-satisfied through the formation of the second generation of planetesimals. Past this stage, the orbital lifetime, as determined from equations (9) and (41), becomes

$$\tau \sim \frac{8}{3C_D}\left(\frac{\rho_p}{\rho_g}\right)\left(\frac{a\Omega}{c}\right)^3 \frac{r}{c} \sim 6 \times 10^5 \; r_5/C_D \qquad (47)$$

where the particle radius r_5 is expressed in units of kilometers. Comparison of equations (45) and (47) reveals that at each stage of accretion the survival time exceeds the growth time by at least two orders of magnitude.

IV. DISCUSSION

There are two related uncertainties which plague any attempt to present a detailed account of the early stages of planetary accretion. The first of these, to which we have previously referred, is the question of the number of nucleation sites that form during the condensation of minerals from the gaseous phase. If the number of independent nucleation sites is so small that the vapor phase is not seriously depleted in the time it takes the particles to gravitationally settle into the equatorial plane, the resulting particles have radii several centimeters in size and the settling time is about ten years. On the other hand, if the number of nucleation sites is so large that the vapor phase is exhausted before appreciable settling takes place, the resulting dust particles may be very much smaller and the corresponding settling time much longer. A related question is the relative rate of cooling of the preplanetary nebula to the settling time of the dust particles. If the cooling time is short compared to the settling time, the chemical composition of the dust disk reflects typical cosmic abundances. However, if the cooling time is longer than the settling time, chemical fractionation occurs at the earliest stage of planetary accretion.

Of the two problems discussed above, the question of the number of nucleation sites is the more fundamental. Because it directly bears on the size and hence the settling time of the dust particles, it sets the time scale to which the cooling time must be compared. It also indirectly affects the cooling time itself, since the opacity of the nebula depends upon the number and size distribution of the dust grains.

Another problem worth mentioning is that gravitational instabilities will begin to grow in the dust disk as soon as its vertical thickness is less than λ_c. Thus, our discussion, in terms of the dispersion relation for a thin disk, is an oversimplification of the true situation. Fortunately, the time scale for growth of these instabilities is identical to that for the thinning of the disk. The major new feature introduced by the finite thickness of the disk is just a decrease of the growth rate of the first generation planetesimals from $2\pi(G\sigma_p/\lambda)^{1/2}$ to $2\pi(G\sigma_p/\lambda_c)^{1/2}$. The calculated masses of the objects are not affected by the finite thickness of the disk.

The main contribution of this investigation is the demonstration that sizable planetesimals can accrete directly from dust grains by means of gravitational instabilities. Thus, the fate of planetary accretion no longer appears to hinge on the stickiness of the surfaces of dust particles. Although we have dismissed the sticking of dust grains as unnecessary to the planetary accretion process, there is a more fundamental reason for disregarding it altogether. That is, even if the dust grains tended to stick together upon impact, the growth of solid bodies by this process would be much slower than by the gravitational instabilities we have described.

This research was supported in part by NASA NGL 05-002-003.

REFERENCES

Chandrasekhar, S., 1955, Vistas in Astronomy, Vol. I, 344.

Chandrasekhar, S., 1961, Hydrodynamic and Hydromagnetic Stability, Oxford University Press, Oxford, p. 491.

Goldreich, P. and Lynden-Bell, D., 1965, "Gravitational Stability of Uniformly Rotating Disks", M. N., 130, 97.

Goldreich, P. and Lynden-Bell, D., 1965, "Spiral Arms as Sheared Gravitational Instabilities", M. N., 130, 125.

Hoyle, F., 1946, "On the Condensation of the Planets", M. N., 106, 406.

Jeffreys, H., 1959, The Earth, Cambridge University Press, Cambridge, p. 241.

Kuiper, G. P., 1951, "On the Origin of the Solar System", Proc. Nat. Acad. Sci., 37, 1.

Larimer, J. W., 1967, "Chemical Fractionations in Meteorites - I. Condensation of the Elements", Geochimica et Cosmochimica Acta, 31, 1215.

Larimer, J. W. and Anders, E., 1970, "Chemical Fractionations in Meteorites - III. Major Element Fractionations in Chondrites", Geochimica et Cosmochimica Acta, 34, 367.

Lewis, J. S., 1972, "Low Temperature Condensation from the Solar Nebula", Icarus, 16, 241.

Lyttleton, R. A., 1972, "On the Formation of Planets from a Solar Nebula", M. N., 158, 463.

Lord, H. C., III, 1965, "Molecular Equilibria and Condensation in a Solar Nebula and Cool Stellar Atmosphere", Icarus, 4, 279.

Polyachenko, V. L. and Fridman, A. M., 1972, "The Law of Planetary Distances", Soviet Astronomy, 16, 125. (Translation from Astronomicheskii Zhurnal, 49, 157.)

Toomre, A., 1964, "On the Gravitational Stability of a Disk of Stars", Ap. J., 139, 1217.

Urey, H. C., 1966, "Chemical Evidence Relative to the Origin of the Solar System", M. N., 131, 199.

Urey, H. C., 1972, "Evidence for Objects of Lunar Masses in the Early Solar System", The Moon, 4, 383.

PART 2. TIDAL FRICTION AND GENERALIZED CASSINI'S LAWS IN THE SOLAR SYSTEM

I. INTRODUCTION

There exists in the solar system an abundance of rotating objects located in orbits that undergo precession. Virtually every planet and satellite fits this description to some degree. For instance, the current rate of change of the longitude of the earth's node on the fixed ecliptic implies an orbit precession period on the order of 70,000 years (Brouwer and Clemence, 1961). This motion is produced by the perturbations of other planets with orbit planes slightly inclined to the ecliptic. A much more rapid precession is realized by the lunar orbit normal which is induced by solar perturbations to revolve about the normal to the ecliptic in only 18.6 years.

With the motion of the orbit plane, the obliquity, ϵ, of the spinning object (the angular separation of its spin axis and the orbit normal) becomes a function of time. Indeed, if a spin axis is nearly fixed in space and separated by an angle δ from the normal, $\hat{k}$, of an invariable plane about which the orbit normal $\hat{n}$ describes a circular motion with a constant inclination i; then the amplitude of the variation of the obliquity, $\Delta\epsilon$, will be equal to 2i if $\delta > i$ or 2δ if $\delta < i$. In fact, it is well known that the obliquity of the earth has a small time dependent contribution, i.e., $\epsilon_\oplus = 23^\circ 27' 8''.26 - 46''.84T$ to first order in T measured in centuries (Allen, 1963). For most of the planets, this effect is nearly negligible compared to the obliquity itself because planetary orbital inclinations are small (Table 1). However, Mercury, Pluto, and to some extent Venus, are exceptions. Their orbits, as well as the orbits of all the satellites in the solar system, vary their orientation in space by a sufficient amount to make this potential change in the obliquities of these objects significant. The most catastrophic

TABLE 1

INCLINATION OF PLANETARY ORBITS

Planet	Inclination to Ecliptic
Mercury	7° 0' 10.6"
Venus	3° 23' 37.1"
Mars	1° 51' 1.1"
Jupiter	1° 18' 31.4"
Saturn	2° 29' 33.1"
Uranus	0° 46' 20.9"
Neptune	1° 46' 45.3"
Pluto	17° 8' 44 "

example of this is afforded by the satellite system of Uranus. The obliquity of Uranus is about 98°, and it has a contingent of five satellites all with orbit planes nearly coincident with the planet's equator plane. Solar torque exerted on this system causes a precession of the planet's spin axis with a time scale on the order of 10^8 years (see Section III). It is apparent that the satellite orbits could remain equatorial only if they partake of the motion of the equator plane of their primary (Goldreich, 1965). This forces one to conclude that if at one instant in time a satellite's obliquity was zero and its spin axis remained fixed in space, then half a period later the obliquity would be $\sim 164°$ and the satellite would be retrograde! (Note: since Uranus rotates retrograde, $\Delta\epsilon \sim 2(\pi - \theta)$ where θ is $\sim 98°$.) One might argue that the strong tidal friction effects accompanying the distortion of the figure of the satellite by the gravitational field of Uranus could, in addition to slowing the satellite's angular velocity to a sychronous value, decay any nonzero obliquity in a time short compared to 10^8 years. However, we shall find that once the spin axis of such a satellite has been driven in the direction of its orbit normal by tidal friction,

this mechanism is no longer required to maintain this condition in spite of the continued movement of the orbit normal. Instead, purely conservative gravitational forces can constrain the spin axis to follow the orbit normal in space.

A planet's (or satellite's) spin vector would remain fixed in inertial space in the presence of an external central gravitational field only if the planet were perfectly spherical and hence felt no gravitational torques. In reality, objects in the solar system are asymmetrical. This is often due to hydrostatic flattening as in the case of the earth, $(C-A)/C = 3.27 \times 10^{-3}$, (Munk and MacDonald, 1960); but it can also be due to an intrinsic asymmetry as in the case of the moon, $(C-A)/C = 6.2 \times 10^{-4}$ (Allen 1963). Even if the earth's rotation ceased, there would still be a nonhydrostatic component on the order of $(C-A)/C \sim 10^{-5}$ (Goldreich and Toomre, 1969). The attraction of the sun (planet) for the figure of a planet (satellite) exerts a couple on it. Under its influence, the spin vector attempts to revolve about the instantaneous orbit normal. Thus, for example, the combined influence of the lunar and solar attraction for the earth's equatorial bulge causes the well known precession of the equinoxes with a period of 27,000 years. It is this phenomenon which in some cases enables a spin axis to follow an orbit normal. In Sections II and III of this paper, we shall demonstrate that the spin axis maintains a nearly constant angular separation from an axis $\hat{\xi}$ which remains coplanar with $\hat{k}$ and $\hat{n}$ during the motion of the latter. The location of $\hat{\xi}$ depends critically on the ratio of the spin and orbit precession periods. Provided the spin axis precession period is much shorter than the period of orbit precession, $\hat{\xi}$ remains close to $\hat{n}$ and the obliquity is virtually a

constant. This is certainly the case for the satellites of Uranus, as well as for the other equatorial satellites in the solar system. (For the earth, however, the spin precession period is not short enough to suppress the small variation in the obliquity mentioned above.)

In this paper, we treat the motions of Mercury, Venus, and all solar system satellites with the exceptions of the small outer objects orbiting Jupiter, Saturn, and Neptune. It is quite likely that all of the objects treated in this paper have been strongly de-spun by tidal friction since the origin of the solar system. Although the conservative forces described above produce a precession of the spin axis, $\hat{s}$, about the vector $\hat{\xi}$, these forces supply no constraints to the radius of the precessional cone $\theta = \cos^{-1}(\hat{\xi} \cdot \hat{s})$. We shall find in Section IV that tidal friction most likely determines this value by driving the spin axis coincident with $\hat{\xi}(\theta \rightarrow 0)$ in a time comparable to that required to decay the spin to a sychronous value. The location of this axis is determined for several solar system objects in Section III under the assumptions of hydrostatic flattening and for (C-A)/C on the order of the lunar value. These objects thus exhibit a generalization of Cassini's laws for the moon (Cassini, 1693) with the spin axis, the orbit normal, and the normal to the invariable plane remaining always coplanar. This motion has previously been suggested for Mercury by Colombo (1966) and later by Peale (1969), and we offer additional support for their proposal here.

We devote Section V to the influence of the 3/2 resonance state of Mercury on the tidal decay of its obliquity. Section VI deals with the rotation of Venus, the only object in this paper with a final rotation state that cannot be explained by tidal friction. If, as advanced by Goldreich

and Peale (1970), friction at the boundary between a solid mantle and a liquid core similar to that of the earth stabilizes the retrograde motion of this planet, then we believe the spin vector should lie one or two degrees short of 180°, because the oblateness of the planet is insufficient for $\hat{\xi}$ to be parallel to the orbit normal. Finally, Section VII concludes the paper with a summary of the results obtained.

II. EQUATIONS

Consider a spinning object orbiting a primary with an orbit plane undergoing precession. Our purpose is to derive the dynamical equations governing the time evolution of this object's obliquity, i.e., the angular separation between its spin and orbit axes. We begin by reviewing the nature of the orbit precession for various processes operating in the solar system. Following this, the precession of the secondary's spin axis is introduced into the problem. Finally, in a coordinate system rotating with the orbit plane, the Hamiltonian for the spin motion is derived.

a) Orbit Precession

We shall separately examine three modes of orbit precession. The causal agents of these modes are (1) a second orbiting body, (2) an oblate primary, and (3) locking of the orbit plane to the equator plane of a primary experiencing precession. (See Figure 1).

Let m and a_1 be the mass and semimajor axis of the object under investigation. Let a second object of mass $M_s >> m$ be located in an orbit with a semimajor axis $a_2 >> a_1$ and inclined to the first by an angle, i_s. For simplicity, we take the orbits to be circular. The disturbing function felt by m due to M_s is given by

$$R = GM_s \{ 1/\Delta - (a_1/a_2^2) \cos S\}$$

$$\Delta^2 = a_1^2 + a_2^2 - 2a_1 a_2 \cos S$$

(Brouwer and Clemence, 1961a). The angle S is the angular separation of the planets,

$$\cos S = \cos^2 i_s/2 \cos(u_2 - u_1) + \sin^2 i_s/2 \cos(u_2 + u_1)$$

where u_1 and u_2 are the angular positions of the bodies measured along

Fig. 1. A composite schematic illustration depicting the precession of the orbit plane of a secondary, m, by (1) another orbiting body, M_s, and (2) an oblate primary, M_p. In the text, these modes are considered separately. Also shown is the precession of the secondary's spin axis, $\hat{s}$.

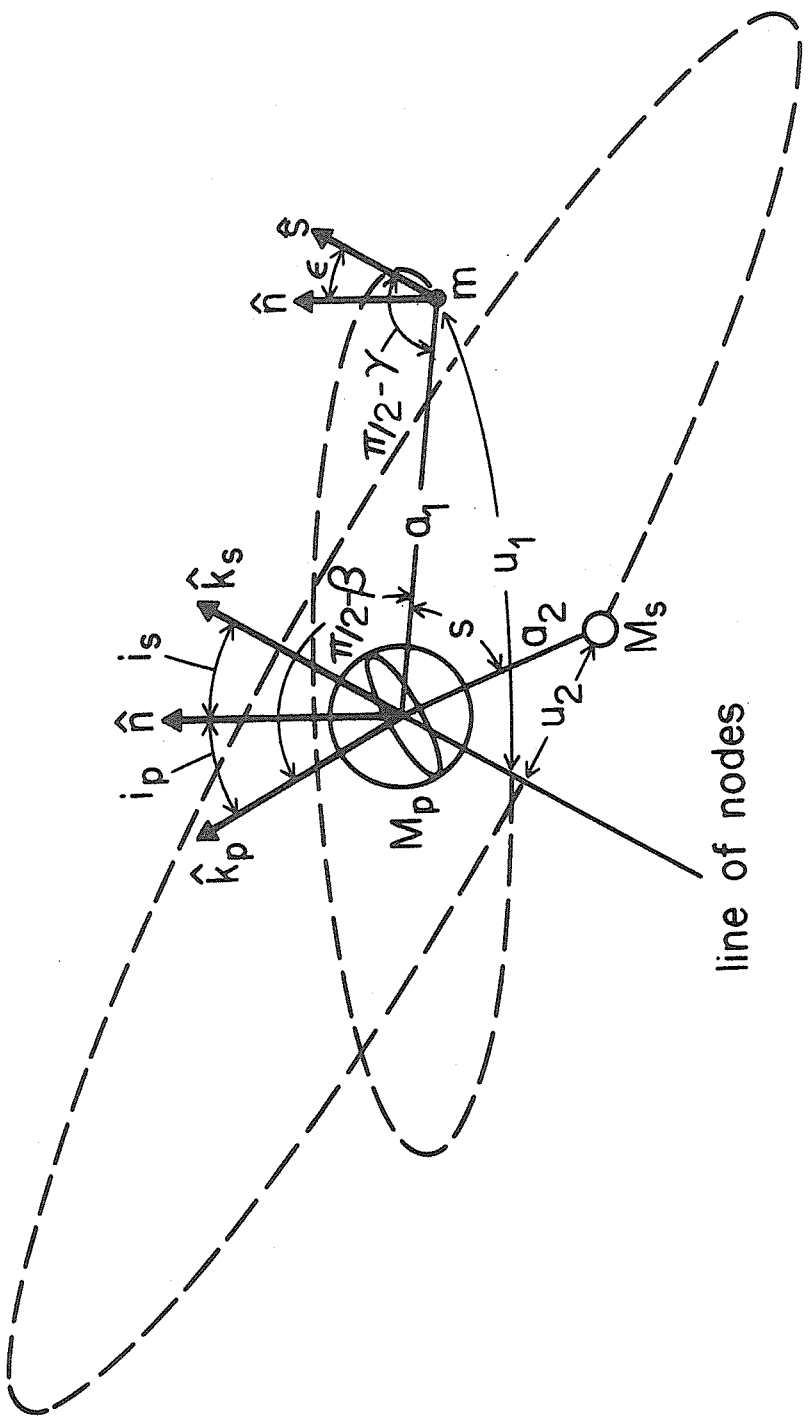
$\hat{s}$
ϵ
$\hat{n}$
m
$\pi/2-\gamma$
a_1
u_1
$\hat{k}_s$
$\pi/2-\beta$
s
a_2
M_s
i_s
$\hat{n}$
i_p
u_2
M_p
$\hat{k}_p$
line of nodes

their respective orbit planes relative to the ascending node of m on the orbit of M_s. Averaging over the orbital periods of both planets yields the secular disturbing function which to second order in i_s is,

$$\bar{R} = \frac{GM_s}{a_2}\left\{\frac{1}{2}b^{(0)}_{1/2} - \frac{1}{2}\frac{a_1}{a_2}b^{(1)}_{3/2}\sin^2 i_s/2\right\} . \qquad (1)$$

The quantities $b^{(j)}_s$ are Laplace coefficients given by

$$\frac{1}{2}b^{(j)}_s = \frac{(s)_j}{j!}\left(\frac{a_1}{a_2}\right)^j F[s, s+j, j+1; (a_1/a_2)^2]$$

where $(s)_j$ is the Pochhammer symbol and F is the hypergeometric function. Differentiation of this quanitity with respect to i_s and subsequent multiplication by m yields a torque which can then be equated to the time rate of change of the orbital angular momentum, $\bar{L}_o$,

$$d\bar{L}_o/dt = \frac{1}{4}\frac{GM_s m}{a_2}\frac{a_1}{a_2}b^{(1)}_{3/2}(\hat{n}\times\hat{k}_s) . \qquad (2)$$

The unit vectors $\hat{n}$ and $\hat{k}_s$ are the orbit normals of m and M_s respectively. Taking the dot product of $\hat{n}$ with this equation reveals that the magnitude of the angular momentum is a constant, $L_o = m(GM_p a_1)^{\frac{1}{2}}$. The mass of the primary has been denoted by M_p. Dividing equation (2) by L_o yields the time rate of change of the orbit normal,

$$d\hat{n}/dt = \Omega_s(\hat{k}_s \times \hat{n}). \qquad (3)$$

Since $M_s \gg m$, $\hat{k}_s$ is assumed fixed in space and the solution is uniform precession of $\hat{n}$, i.e., $\hat{n}$ describes a circular motion about $\hat{k}_s$ while maintaining a constant inclination, i_s. The precession frequency is given by

$$\Omega_s = -\frac{\pi}{2P}\left(\frac{M_s}{M_p}\right)\left(\frac{a_1}{a_2}\right)b^{(1)}_{3/2} \qquad (4)$$

where P is the orbital period of m.

Let i_p be the inclination of the orbit of m to the equator plane of the primary. If the primary is oblate, the disturbing function due to the attraction of m for the primary's figure is

$$U = -(G/a_1^3)\ (C_p - A_p)\ P_2(\sin\beta)$$

(Brouwer and Clemence, 1961a). It has been assumed that the primary is axisymmetric with C_p and A_p representing the maximum and minimum moments of inertia. The symbol P_2 denotes a Legendre polynomial of the second order. Terms of higher order have been neglected. The angle β is the latitude of m as seen in a coordinate system centered on M_p with its z-axis coincident with its spin axis, $\hat{k}_p$, and its x-axis pointing toward the node of m on the equatorial plane of the primary. If Θ measures the angular separation of m from the x-axis, then $\sin\beta = \sin i \sin\Theta$. Upon averaging over an orbit the surviving secular contribution becomes,

$$\langle U \rangle = (G/a_1^3)\ (C_p - A_p) \left\{ \frac{3}{4} (\hat{n} \cdot \hat{k}_p) - \frac{1}{4} \right\} . \qquad (5)$$

This leads to an equation analogous to (3)

$$d\hat{n}/dt = \Omega_p (\hat{k}_p \times \hat{n}) . \qquad (6)$$

Again considering $\hat{k}_p$ fixed, we obtain uniform precession with a constant inclination i_p and a frequency

$$\Omega_p = \frac{-3\pi}{P} \left(\frac{C_p - A_p}{M_p R_p^2} \right) \left(\frac{R_p}{a_1} \right)^2 (\hat{n} \cdot \hat{k}_p) \qquad (7)$$

where R_p is the radius of M_p.

Examples of both types of precession thus far considered are present in the solar system. Of the objects treated in this paper, orbit precession

by a second orbiting body occurs for the moon, Mercury, and Venus. For the lunar orbit, it is the sun which plays the role of M_s while the orbits of Mercury and Venus experience precession as a result of the gravitational perturbations of the other planets. For Triton, on the other hand, it is the torque arising from the hydrostatic flattening of Neptune which is important. Iapetus is an interesting intermediate case, because the torques due to the sun and to the equatorial bulge of Saturn (together with the pull of the large satellite Titan) are comparable. The orbit normal for Iapetus can revolve about neither $\hat{k}_s$ nor $\hat{k}_p$. Instead, nearly uniform precession is executed about a third vector, $\hat{k}'$, which is coplanar with the other two and located about midway between (Tisserand, 1896).

Most satellites in the solar system have orbit planes lying in, or nearly in, the equator plane of their primary. These include J5 and the Galilean satellites of Jupiter, the inner satellites of Saturn, as well as the systems of Mars and Uranus. For all of these objects, it is the torque from the figure of the primary which is the most important. However, due to the low inclination, the amplitude for the variation of $\hat{n}$ is small, $\sim 2i$. On the other hand, it is clear that if these orbits are to remain equatorial for the duration of the solar system, they must possess the ability to follow any change in the position of the primary's equator (Goldreich, 1965). Above we considered $\hat{k}_p$ to be fixed, an assumption quite adequate over short time scales on the order of the orbit precession period, $P_0 = 2\pi/|\Omega_p|$. On a longer time scale, there is an additional precession of the primary's spin axis about its own orbit normal exemplified by the 27,000 year advance of the equinoxes on earth. Thus, this furnishes a third mode of orbit

precession experienced among solar system objects. Though of low frequency, the amplitude (which is equal to twice the obliquity of the primary) can be quite large.

Depending on which of the three types of precession is produced, we shall take the following expression for $\hat{n}(t)$,

$$\hat{n} = \cos i\hat{k} + \sin i\,[\cos(\Omega t)\hat{x} + \sin(\Omega t)\hat{y}] \qquad (8)$$

i.e., uniform precession where $\hat{k}$, i, and Ω are chosen appropriately for each object. Unit vectors $\hat{x}$ and $\hat{y}$ are chosen so as to make an orthogonal set.

b) Spin Precession

If the spin axis, $\hat{s}$, of m remained fixed in inertial space, the obliquity of the body, $\epsilon = \cos^{-1}(\hat{s}\cdot\hat{n})$, would be determined as a function of time once the precession of $\hat{n}$ was described. This, of course, is not the situation. The spin axis of an object in an external gravitational field will not remain fixed if the object is oblate. A certain amount of oblateness always accompanies a spinning object due to hydrostatic flattening and many objects (such as the moon) probably sustain an intrinsic oblateness considerably larger than the hydrostatic value. The formalism for the precession of the spin axis has already been developed in equation (5). If we interchange the roles of m and M_p by establishing a coordinate system on m with the z-axis coincident with $\hat{s}$ and the x-axis pointing toward the ascending node of M_p on the equatorial plane of m, we can write the disturbing function felt by M_p as

$$V = \frac{-G}{a_1^3}(C_s - A_s)\,P_2(\sin\gamma)$$

where we have again assumed axial symmetry. The principal moments of inertia are those of m, while γ is the latitude of M_p given by $\sin\gamma =$

$\sin\epsilon \sin\Theta'$ where Θ' is the angular separation of M_p from the x-axis. Averaging over an orbit produces the secular part,

$$\langle V \rangle = \frac{G}{a_1^3} (C_s - A_s) \left\{ \frac{3}{4} (\hat{s} \cdot \hat{n})^2 - \tfrac{1}{4} \right\} . \qquad (9)$$

Multiplying this by M_p produces an expression which, when differentiated, yields a torque analogous to that obtained from (5). However, this torque causes the precession of the spin axis of m instead of its orbit plane. (In both cases, the bulk of the angular momentum resides in the motion of M_p which is little affected by the mutual torques between it and m.)

Although $\langle U \rangle$ and $\langle V \rangle$ are of the same form, there is an important difference. Whereas, in the former, $\hat{k}_p$ was considered fixed in space; in the latter, $\hat{n}$ has an explicit time dependence given by equation (8). As a consequence, *although the Hamiltonian for the spin vector can be identified as the energy by virtue of the lack of time dependence of the generalized coordinates,*

$$H = \tfrac{1}{2} \bar{s} \cdot \bar{L}_s + M_p \langle V \rangle ,$$

this energy is not a constant of motion, i.e., $dH/dt = \partial H/\partial t \neq 0$ (Goldstein, 1950). Here $\bar{L}_s$ represents the spin angular momentum of m and $\bar{s} = \omega \hat{s}$, where ω is the spin frequency. We can simplify this problem by performing a canonical transformation to a new system rotating with the orbit plane. Let $\hat{x}'$, $\hat{y}'$, and $\hat{z}'$ denote the principal axes fixed in the planet and located by Euler angles θ, Ψ, and Υ with respect to inertial space vectors $\hat{x}$, $\hat{y}$, $\hat{z}$ (Figure 2). The orbit normal $\hat{n}$ revolves clockwise about $\hat{k}$ maintaining a constant inclination i. We can eliminate the time dependence of $\hat{n}$ by transforming to a coordinate system $q_i' = f_i(q_j)$ in which $\hat{n}$ is constant, i.e., rotating about $\hat{z}$ with angular

Fig. 2. The orientation of the principal axes of the secondary, (x',y',z'), with respect to the inertial space vector (x,y,z). Angles θ, φ, and ψ are Euler angles. Unit vectors $\hat{s}$ and $\hat{n}$ locate the spin axis and the orbit normal of the secondary respectively. The vector $\hat{k}$ is normal to the invariable plane.

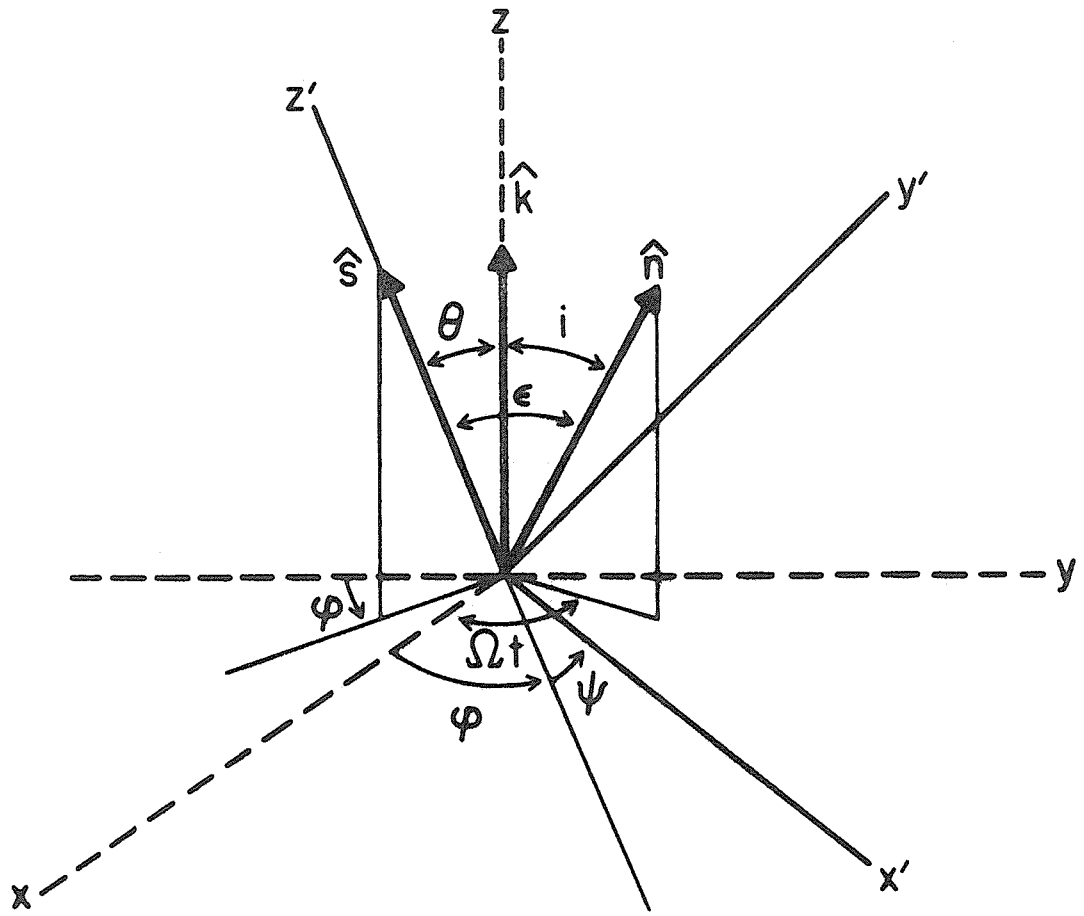
z
z′
k̂
y′
ŝ
n̂
θ
i
ϵ
y
φ
Ωt
ψ
φ
x
x′

velocity Ω

$$\varphi' = \varphi - \Omega t \quad , \quad \theta' = \theta \quad , \quad \Psi' = \Psi \quad .$$

This is a simple point transformation and is, therefore, canonical. We wish to obtain the new Hamiltonian K in the rotating system. This is given in terms of the old Hamiltonian by

$$K = H + \partial F/\partial t$$

where F is the generating function of the transformation (Goldstein, 1950). The generating function we require is of the type $F_2(q,p')$

$$F_2 = \sum p_i' f_i (q_i) = \theta p_\theta' + \Psi p_\psi' + (\varphi - \Omega t)\, p_\varphi' \quad .$$

This gives us $q_i' = \dfrac{\partial F_2}{\partial p_i'} = f_i$ as required, and we also find that the momenta transform identically

$$p_i = \partial F_2/\partial q_i = p_i' \quad .$$

Substituting F_2 into K, we obtain

$$K = H - \Omega p_\varphi' \quad . \tag{10}$$

Now since p_φ' is simply the component of the planet's spin angular momentum, $\bar{L}_s$, in the direction of $\hat{k}$, we can write

$$K = \tfrac{1}{2}\bar{s}\cdot\bar{L}_s - (C_s - A_s)n^2 \left\{ \frac{3}{4}(\hat{n}\cdot\hat{s})^2 - \tfrac{1}{4} \right\} - \Omega(\bar{L}_s\cdot\hat{k}) \ ,$$

where n is the mean motion. We make the further simplifying assumption that $\bar{L}_s = C_s\bar{s}$, that is, we neglect any nonprincipal axis rotation. Such rotation would induce internal energy dissipation as a result of the wandering spin axis which would damp out this motion and quickly drive the spin axis coincident with the principal moment of inertia. We have for K;

$$K = \tfrac{1}{2}C_s\omega^2 - (C_s - A_s)\, n^2 \left\{ \frac{3}{4}(\hat{n}\cdot\hat{s})^2 - \tfrac{1}{4} \right\} - C_s\omega\Omega(\hat{s}\cdot\hat{k}) \quad . \tag{11}$$

We note that $dK/dt = \partial K/\partial t = 0$ so that K is a constant of motion. On the other hand, because the transformation contains time, K cannot be identified as the total energy. Nevertheless, the effective torque exerted on the planet in the rotating reference frame can be found from differentiating the pseudo-potential,

$$\bar{\tau} = -\frac{3}{2}(C_s - A_s)\, n^2 (\hat{n}\cdot\hat{s})(\hat{n}\times\hat{s}) - C_s\omega\Omega(\hat{k}\times\hat{s}) = d\bar{L}_s/dt \quad . \tag{12}$$

This is a first order vector differential equation for the momentum $\bar{L}_s$. We first observe that from the dot product of $\hat{s}$ with equation (12), $L_s = C_s\omega$ is also a constant of motion. Equation (12) then becomes

$$d\hat{s}/dt = -\alpha(\hat{n}\cdot\hat{s})(\hat{n}\times\hat{s}) - \Omega(\hat{k}\times\hat{s}) \tag{13}$$

where we have designated,

$$\alpha = \frac{3}{2}\,\frac{(C_s - A_s)}{C_s}\,\frac{n^2}{\omega} \quad . \tag{14}$$

We could have written this equation down directly by equating $d\bar{L}_s/dt$ to the torque resulting from equation (9), and then transforming to the rotating coordinate system by replacing the time derivative by the operator $\{d/dt + \Omega\hat{k}\times\}$. The more circuitous route of first establishing the Hamiltonian was chosen because extensive use shall be made of this quantity in the next section. We finish this section by finding an approximate time dependent solution for the obliquity in the case where the spin precession period $P_s = 2\pi/\alpha|\cos\epsilon|$ is much shorter than the orbit precession period $P_0 = 2\pi/|\Omega|$. To solve equation (13), it is convenient to reorient our rotating coordinate system so that $\hat{n}$ is in the $\hat{z}$ direction and $\hat{k}$ lies in the $\hat{y}$, $\hat{z}$ plane. The obliquity ϵ is now the colatitude. Resolving $\hat{k}$ and $\hat{s}$ into

component vectors results in

$$\hat{k} = \sin i\,\hat{y} + \cos i\,\hat{z}$$

$$\hat{s} = \sin\epsilon\cos\varphi\,\hat{x} + \sin\epsilon\sin\varphi\,\hat{y} + \cos\epsilon\,\hat{z}$$

where φ is the azimuthal angle measured from the x-axis. Substitution of these into equation (13) leads, after manipulation, to the following equations:

$$d\epsilon/dt = -\Omega \sin i \cos\varphi \tag{15}$$

$$d\varphi/dt = -\Omega\cos i - \alpha\cos\epsilon + \Omega \sin i \sin\varphi \cot\epsilon\ . \tag{16}$$

We can use these two equations to demonstrate our contention that ϵ is nearly constant when $P_s \ll P_o$. If $|\Omega/\alpha| \ll 1$, we can integrate the second equation to find

$$\varphi \approx \varphi_o - (\alpha\cos\epsilon)t\ . \tag{17}$$

Using this expression in $d\epsilon/dt$ gives

$$\epsilon \sim \epsilon_o + (\Omega/\alpha)\sin i \sec\epsilon_o\ [\sin(\varphi_o - \alpha t\cos\epsilon_o) - \sin\varphi_o]\ . \tag{18}$$

Since $P_s/P_o \ll 1$, ϵ remains nearly equal to ϵ_o in spite of the precession of $\hat{n}$.

III. GEOMETRY

In this section the geometry of the motion will be considered. A lucid description can be given if time is eliminated from the equations. This can be done from equations (15) and (16) followed by integration or, alternatively, we can simply use the Hamiltonian K. Since L is constant it follows that $C\omega^2 = L^2/C$ must be constant. Rearranging K, we find,

$$\begin{aligned} E &= \left\{K - \frac{1}{2} C\omega^2 - \tfrac{1}{4}(C-A) n^2\right\}/C\omega \\ &= -\frac{\alpha}{2} (\hat{n}\cdot\hat{s})^2 - \Omega(\hat{k}\cdot\hat{s}) \end{aligned} \tag{19}$$

where E is also a constant. When $\hat{n}$, $\hat{k}$, and $\hat{s}$ are again resolved into the unit vectors as above, E takes the form

$$E = -\frac{\alpha}{2} \cos^2\epsilon - \Omega \{\sin i \sin\epsilon \sin\varphi + \cos i \cos\epsilon\} \quad . \tag{20}$$

This expression contains a term first order in i that varies with the angle φ. However, this is not the best coordinate system to illustrate the nature of the solution. Suppose, instead, that the z-axis is located in the plane of the vectors $\hat{n}$ and $\hat{k}$, but inclined to $\hat{n}$ by an angle ξ. We shall refer to this axis as the ξ-axis (Figure 3). In this case,

$$\begin{aligned} E/\alpha = -\tfrac{1}{2} \{&\cos^2\xi \cos^2\theta - 2\cos\xi \sin\xi \cos\theta \sin\theta \sin\varphi \\ &+ \sin^2\xi \sin^2\theta \sin^2\varphi\} - \frac{\Omega}{\alpha} \{\cos(i-\xi) \cos\theta + \sin(i-\xi) \sin\varphi \sin\theta\} \quad . \end{aligned} \tag{21}$$

We now define the value of ξ by the following equation,

$$\alpha \sin 2\xi \cos\theta = 2\Omega \sin(i-\xi) \quad . \tag{22}$$

(Note that ξ is not a constant, but is a function of θ.) Using this definition,

Fig. 3. The coordinate system rotating with the orbit plane with the z-axis in the direction of the auxiliary vector $\hat{\xi}$. Vectors $\hat{n}$ and $\hat{k}$ are fixed and located in the (y,z) plane.

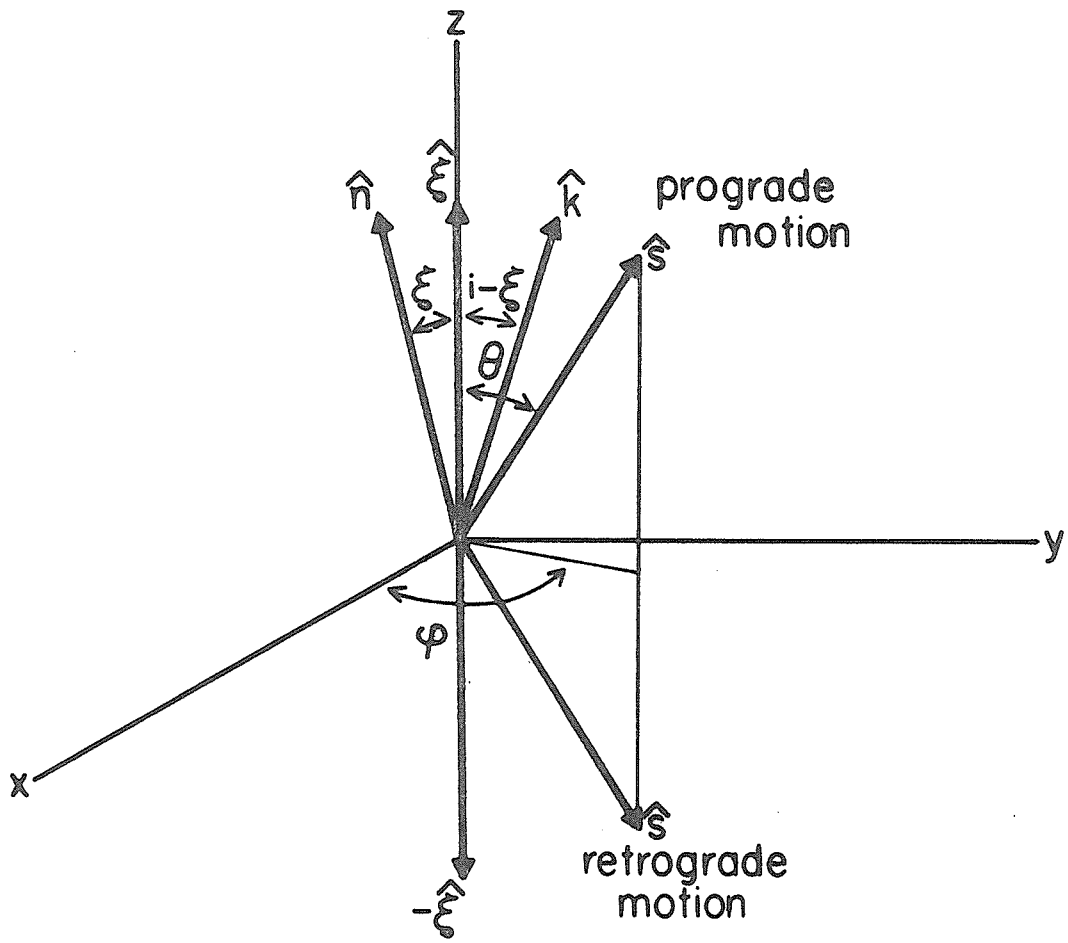
z
$\hat{\xi}$
$\hat{n}$
$\hat{k}$
prograde
motion
$\hat{s}$
ξ
i-ξ
θ
y
φ
x
$\hat{s}$
retrograde
motion
$-\hat{\xi}$

$$E/\alpha = -\tfrac{1}{2}\cos^2\xi\cos^2\theta - \frac{\Omega}{\alpha}\cos(i-\xi)\cos\theta - \tfrac{1}{2}\sin^2\xi\sin^2\theta\sin^2\varphi. \qquad (23)$$

a) Prograde Rotation

For the prograde solution, we begin by defining E(0) by

$$E(0)/\alpha = -\tfrac{1}{2}\cos^2\xi - \frac{\Omega}{\alpha}\cos(i-\xi) \quad . \qquad (24)$$

Subtracting equation (24) from (23) and using the half-angle formulae for $\sin\theta/2$ yields,

$$\sin^4\theta/2 - (1+B)\sin^2\theta/2 + A = 0 \qquad (25)$$

where

$$B = \frac{(\Omega/\alpha)\cos(i-\xi)}{1 - \sin^2\xi(1+\sin^2\varphi)} \qquad A = \frac{[E - E(0)]/2\alpha}{1 - \sin^2\xi(1+\sin^2\varphi)} \quad . \qquad (26)$$

The solution is

$$\sin^2\theta/2 = \tfrac{1}{2}(1+B)\left\{1 - [1 - 4A/(1+B)^2]^{\frac{1}{2}}\right\} \qquad (27)$$

where we have picked that root which vanishes as $E \to E(0)$. This can be simplified if we restrict the discussion to values of θ for which $\sin\theta/2 \approx \frac{1}{2}\sin\theta$ is a good approximation. In this case, $\sin^4\theta/2$ can be neglected in equation (25) to give $\sin^2\theta/2 \approx A/(1+B)$. Substituting for A and B, taking the square root, and retaining terms to second order,

$$\sin\theta/2 \approx \left[\frac{[E - E(0)]/2\alpha}{1+\frac{\Omega}{\alpha}\cos(i-\xi)}\right]^{\frac{1}{2}} \left\{1 + \frac{\sin^2\xi\,(1+\sin^2\varphi)}{2[1+\frac{\Omega}{\alpha}\cos(i-\xi)]}\right\} \quad . \qquad (28)$$

(This expression diverges for $(\Omega/\alpha)\cos(i-\xi) = -1$ in which case the approximation is no longer valid. Actually, equation (24) is not obtained by evaluating equation (23) at $\theta = 0$. Such an evaluation would contain $\xi_0 = \xi(\theta = 0)$ instead of ξ. However, the difference between E(0) as defined and equation (23) with $\theta = 0$ is of higher order than we are considering and can be neglected.) The important observation to make is that the

motion is one in which θ remains constant except for a small fractional change that is second order in $\sin\xi$. This means that the spin vector revolves with a nearly constant angular separation about an axis, $\hat{\xi}$, inclined by the angle ξ to the orbit normal $\hat{n}$. The vectors $\hat{n}$, $\hat{k}$, and $\hat{\xi}$ are coplanar. The location of the ξ-axis is given by equation (22). It follows that ξ is very nearly constant if θ is.

If ξ is a small angle,

$$\sin \xi \approx \sin i/\{\cos i + (\alpha/\Omega) \cos \theta\} \quad . \tag{29}$$

For objects in prograde orbits, Ω is negative. As $|\Omega/\alpha| \to 0$, $\sin\xi \approx \Omega \sin i/\alpha \cos\theta$, so that ξ approaches zero through negative values. The proper interpretation of negative angles is that $\hat{\xi}$ is inclined to $\hat{n}$ in the direction away from $\hat{k}$. It is now apparent that the obliquity, $\epsilon = \cos^{-1}(\hat{n}\cdot\hat{s})$, is nearly constant for $P_s/P_o \ll 1$ simply as a result of the close proximity of $\hat{\xi}$ to $\hat{n}$. (Triton and the satellites of Uranus are located in retrograde orbits so that $\Omega > 0$. However, since the spins of these objects are undoubtedly retrograde also, the situation is simply inverted from that above, so that the discussion of this section applies. The positive value of $\sin\xi$ for these objects when $\Omega/\alpha \ll 1$ means that $\hat{\xi}$ is inclined to $\hat{n}$ in the direction away from $-\hat{k}$.)

At the other extreme, if $|\Omega/\alpha| \gg 1$, it is clear from equation (22) that $(\xi - i)$ becomes small and we can write,

$$\sin (\xi - i) \approx -\tfrac{1}{2} \sin 2i/\{\cos 2i + (\Omega/\alpha) \sec \theta\} \quad . \tag{30}$$

As $|\Omega/\alpha| \to \infty$, $\sin(\xi - i) \approx -\alpha \cos\theta \sin 2i/2\Omega$. For prograde orbits, $\hat{\xi}$ is inclined to $\hat{k}$ by $(\xi - i)$ in the direction away from $\hat{n}$. (For retrograde orbits $\hat{\xi}$ is inclined to $-\hat{k}$ in the same manner.)

The precession of the spin vector - when viewed down the ξ-axis - is clockwise when $\hat{\xi}$ is close to $\hat{n}$ and counterclockwise if $\hat{\xi}$ is close to $\hat{k}$. Remember that we are in a rotating coordinate system. The counterclockwise

motion when $\hat{\xi}$ is near $\hat{k}$ reflects that fact. Actually, in inertial space the spin axis moves little during the precession of the orbit for this case. The region between $\hat{k}$ and $\hat{n}$ is forbidden to $\hat{\xi}$ for prograde motion. Whenever the spin vector is in this position the clockwise and counterclockwise precessions add, both tending to advance $\hat{s}$ in the x direction (Figure 3). It is clear that $\hat{s}$ could not execute a circular motion about an axis in this region, for return motion in the -x direction would be impossible.

(i) Mercury

Radar measurements indicate that Mercury rotates in a direct sense with a period equal to 2/3 its orbit period, or about 59 days (Pettengill and Dyce, 1965; Goldreich and Peale, 1966, 1968). We now inquire as to the actual location of the ξ-axis. A near constant obliquity imposes the following condition on the oblateness,

$$(C-A)/C \gg \frac{2}{3}\left(\frac{P^2}{DP_0}\right)|\sec\theta| \quad , \tag{31}$$

where P is the orbit period and D the length of day. The appropriate values for Mercury are D/P = 2/3 (resonance), P = 88 days, $P_0 \cong 2.5 \cdot 10^5$ years (Brouwer and Clemence, 1961b) from which is obtained

$$(C-A)/C \gg 9.2 \cdot 10^{-7} \sec\theta \quad .$$

A lower limit for (C-A)/C can be established by calculating this value due to hydrostatic flattening. The principal moments of inertia are given by

$$C = I[1 + (2kR^5/9GI)\omega^2] \tag{32a}$$

$$A = I[1 - (kR^5/9GI)\omega^2] \tag{32b}$$

where k is the fluid Love number, R the planet's radius, ω the spin angular velocity, and I the moment of inertia of the equivalent sphere (Munk and MacDonald, 1960). This gives us

$$(C - A)/C_{min} \approx (k/3K)(\omega/\omega_c)^2 \tag{33}$$

where K is the square of the ratio of the radius of gyration to the planet's radius and $\omega_c^2 = GM/R^3$, M being the planet's mass. For Mercury, $(C-A)/C_{min} \approx (k/3K) \times 10^{-6}$. (For the earth k = .95, K = .335, and $k/3K \approx .95$.) However, it is quite likely that the planet can support a nonhydrostatic oblateness much larger than this. For instance, the moon with about a quarter of the mass of Mercury has an oblateness of 6.2×10^{-4}, while even the earth with $18\frac{1}{2}$ times the mass of Mercury has a nonhydrostatic contribution on the order of 10^{-5}. Recently a similar nonhydrostatic component has been found for Mars (Lorell, et al., 1972). We conclude, therefore, that it is quite likely that the obliquity of Mercury remains very nearly constant during the planet's orbit precession. For $(C - A)/C \approx 10^{-4}$, the ξ-axis is inclined by an amount $\xi \approx -5.6 \sec\theta$ minutes of arc to the orbit normal (Colombo, 1966).

(ii) Moon

The lunar orbit undergoes precession due to solar gravity with a period of 18.6 years while maintaining an inclination of $5^\circ 8'$ to the ecliptic. The oblateness, $(C-A)/C$ has the value 6.2×10^{-4}. This is considerably in excess of the hydrostatic value of $5.6 \times 10^{-6} k$ given by equation (33) with $K \approx 2/5$. As a result, the earth exerts a sufficient torque on the lunar figure to revolve its spin axis with a period of 78.5 years. From equation (30) it can be shown that the ξ-axis is inclined to the normal to the ecliptic, $\hat{k}_{\mathfrak{D}}$, by $1^\circ 35'$ in the direction away from the lunar orbit normal, $\hat{n}_{\mathfrak{D}}$.

(iii) Triton

Triton affords us with a very interesting application. First, unlike Mercury and the moon, the orbit of Triton experiences precession almost exclusively due to the torque arising from the equatorial bulge of its

primary, Neptune. Secondly, the orbit itself is retrograde and very highly inclined - by some 20.1° to the equator plane. If tidal friction has driven the satellite to synchronous rotation, the spin should be retrograde also. Because the rotation and revolution are in the same sense, Triton is correctly treated in this section rather than the following one on retrograde rotation.

Observational evidence indicates that Triton has an orbit precession period on the order of 600 years (Brouwer and Clemence, 1961b). The value for the oblateness of Triton due to hydrostatic flattening with the length of the day set equal to the length of the month is $(C-A)/C \geq 5.5 \times 10^{-4} \rho^{-1} \times (k/3K)$ where ρ is the density of the satellite. Lewis (1971) has suggested that large outer satellites such as Triton may have liquid water-ammonia mantles as a consequence of radioactive heating. If so, then the hydrostatic value would be appropriate. For $\theta = 0$, $k \sim 1.5$, $K \sim 0.4$, $\rho \sim 2$ gm/cm^3, equation (29) would yield $\xi \approx -1.1°$. Hence the spin axis would be able to "follow" the orbit normal rather well. On the other hand, if Triton is solid throughout, the oblateness may be more lunar-like, implying that the ξ-axis would be even closer to the orbit normal, i.e., $\xi \approx -0.6° \sec\theta$.

(iv) Iapetus

The location of the spin axis of Iapetus (Saturn 8) was first considered by Colombo (1966). As mentioned earlier, the near equality of the solar torque to the combined torques of Saturn and Titan make it impossible for the orbit of Iapetus to maintain a constant inclination to either the orbital or equator plane of Saturn. These planes are tilted with respect to each other by 26°44'. As a compromise, the orbit describes a circular path about

a mean pole which has an angular separation of $\sim 14.7^\circ$ from the spin axis of Saturn, but which is coplanar with this axis and Saturn's orbit normal (Tisserand 1896). The orbit normal of Iapetus remains inclined to the mean pole by 8° during its ~3000 year precession period. Iapetus is known to have achieved synchronous rotation from its photometric phase curve. A regular sinusoidal light variation of about two magnitudes has been observed (Widorn, 1950) with a period equal to its orbit period. The hydrostatic value of $(C-A)/C$ from such a spin rate is too small to be of dynamical significance, $\sim 3 \times 10^{-6} \rho^{-1} (k/3K)$. (This is the same order of magnitude as the hydrostatic value obtained for Mercury, except here we are dealing with an orbit that takes about one tenth as long to trace its circular path.) If this value is appropriate for Iapetus, then the ξ-axis lies close to the mean pole, i.e., $\xi \approx 8^\circ$. On the other hand, if a lunar value is more appropriate, $P_s \approx 230$ years and $\xi \approx -0.65^\circ \sec \theta$.

(v) Equatorial Satellites

The orbit planes of equatorial satellites must experience precession with the equator plane of the primary if they are to remain in the equator plane. To determine the ability of a satellite's spin axis to "follow" the orbit normal, we must first ascertain the primary's precession period. It is not sufficient to merely compute the solar torque on the primary. In general, an accompanying entourage of satellites can affect this period in two ways. Those satellites which tend to partake of the precession add their contribution of angular momentum to that of the system. In addition, the solar torque on their orbits is transmitted to the primary and must be added to the solar torque acting on the equatorial bulge. In this situation, the precession period is to be obtained from the expression,

$$T = P\left(\frac{P}{D}\right)\left\{\frac{K + (\omega_c/\omega)\sum_i (m_i/M_p)(a_i/R_p)^{\frac{1}{2}}}{J + \frac{3}{4}\sum_i (m_i/M_p)(a_i/R_p)^2}\right\} \sec \epsilon_p$$

where $(C-A)/C = 2J/3K$, M_p, R_p, ϵ_p, P, and D are the oblateness, mass, radius, obliquity, orbit period and spin period of the primary respectively; while m_i and a_i are the mass and semimajor axis of the i^{th} satellite. On the other hand, if a satellite is not locked to the planet (such as the moon), it assists the sun in exerting a torque on the equatorial bulge. In this case the period is given by,

$$T = P\left(\frac{P}{D}\right)\frac{K}{J}\left\{1 + \sum_i (m_i/M_\odot)(r/a_i)^3\right\}^{-1} \sec \epsilon_p$$

where $M_\odot$ is the solar mass and r the sun-planet distance. Table 2 lists the derived precession periods for the planets

TABLE 2

SPIN PRECESSION PERIODS OF THE PLANETS

Planet	Obliquity[2]	K[2]	J[3]	Precession Period Without Satellites	With Satellites
Mercury[1]	-	-	-	$2.4 \cdot 10^3$	-
Venus	-	~.34	$<7.5 \cdot 10^{-6}$[4]	$>2.5 \cdot 10^4$	-
Earth	23° 27'	.335	$1.64 \cdot 10^{-3}$[2]	$7.4 \cdot 10^4$	$2.7 \cdot 10^4$
Mars	23° 59'	.359	$2.95 \cdot 10^{-3}$	$1.8 \cdot 10^5$	$1.8 \cdot 10^5$
Jupiter	3° 05'	.25	.0296	$1.0 \cdot 10^6$	$4.3 \cdot 10^5$
Saturn	26° 44'	.22	.027	$6.8 \cdot 10^6$	$1.8 \cdot 10^6$
Uranus	97° 55'	.23	.023[5]	$2.1 \cdot 10^8$	$9.7 \cdot 10^7$
Neptune	28° 48'	.29	.007[6]	$7.5 \cdot 10^8$	$2.3 \cdot 10^7$

[1] Computed for $(C-A)/C \sim 10^{-4}$.
[2] Allen, 1963.
[3] JPL Report 32-1306 except where otherwise specified.
[4] Anderson and Efron, 1969.
[5] Optical J .
[6] Brouwer and Clemence, 1961b .

We now compare these periods with those for spin precession of the satellites assuming hydrostatic flattening and sychronous rotation. The expression for the spin precession period can be written

$$P_s = 2(3\pi)^{\frac{1}{2}} \left(\frac{K_s}{k_s}\right)\left(\frac{\rho_s}{\rho_p}\right)(G\rho_p)^{-\frac{1}{2}}\left(\frac{a_s}{R_p}\right)^{9/2} \sec\epsilon$$

where the subscripts s and p denote satellite and primary values respectively. As an estimate, we take $K_s \approx 2/5$, $k_s \approx 1.5$, and $\epsilon \approx 0$, obtaining $P_s = 2\times10^{-4}\,\rho_s\rho_p^{-3/2}(a_s/R_p)^{9/2}$ years. This period is a strongly, monotonically increasing function of the satellite's orbital semimajor axis (measured in units of the primary's radius, a_s/R_p). Hence, the larger the orbit, the more difficult it is for the spin axis to follow the moving orbit normal.

TABLE 3

SPIN PRECESSION PERIODS FOR HYDROSTATICALLY FLATTENED SATELLITES

Outer Equatorial Satellite	a_s/R_p	ρ_p	P_s (years)
Mars, Deimos	6.92	3.97	0.45
Jupiter, Callisto	26.36	1.33	0.93×10^3
Saturn, Hyperion	24.83	0.68	2.1×10^3
Uranus, Oberon	24.69	1.60	5.6×10^2

In Table 3, we have calculated P_s for the outer most equatorial satellite of each system. To be careful not to underestimate the time, ρ_s has been set equal to 3 gm/cm^3. Comparison of the values with Table 2 reveals that for each, $\hat{\xi} \approx \hat{n}$ and the satellite's obliquity will remain nearly constant. It follows that this will also be the situation for the inner satellites.

b) Retrograde Rotation

The rotation of Venus is known to be retrograde. The obliquity is close to 180° (Shapiro, 1967; Carpenter, 1964, 1970). We conclude, therefore, that the approximation $\sin\theta/2 \approx \frac{1}{2}\sin\theta$ is not valid. Instead, we proceed as follows: Let

$$E(\pi)/\alpha = \tfrac{1}{2}\cos^2\xi + \frac{\Omega}{\alpha}\cos(i-\xi) \quad . \tag{34}$$

Subtracting from equation (23) and using the half-angle formulae for cosine,

$$\cos^4\theta/2 - (1-B)\cos^2\theta/2 + A' = 0 \tag{35}$$

where instead of A, we have used

$$A' = \frac{[E - E(\pi)]/2\alpha}{1-\sin^2\xi(1+\sin^2\varphi)} \quad . \tag{36}$$

We now make the approximation $\cos\theta/2 \approx \frac{1}{2}\sin\theta$ which for angles near π is quite good. This enables us to neglect the $\cos^4\theta/2$ term in equation (35) yielding the solution $\cos^2\theta/2 \approx A'/(1-B)$. Substituting for A' and B, taking the square root, and retaining terms up to second order in ξ,

$$\cos\theta/2 \approx \left[\frac{[E - E(\pi)]/2\alpha}{1-\frac{\Omega}{\alpha}\cos(i-\xi)}\right]^{\frac{1}{2}} \left\{1 + \frac{\sin^2\xi\,(1+\sin^2\varphi)}{2\left[1-\frac{\Omega}{\alpha}\cos(i-\xi)\right]}\right\} \quad . \tag{37}$$

We see that θ is again very nearly constant and the motion is precession about the ξ-axis inclined to $\hat{n}$ by ξ given by equation (22). Since the

motion is retrograde, $\cos\theta < 0$ and $\xi > 0$. As $|\Omega/\alpha| \to 0, \xi \to 0$ from above, as $|\Omega/\alpha| \to \infty$, $\xi \to i$ from below. At intermediate values the ξ-axis is always located between $\hat{n}$ and $\hat{k}$, the three vectors being coplanar. This is just the region forbidden to $\hat{\xi}$ in the case of prograde motion. Figure 3 illustrates this situation. The precession always appears counterclockwise looking down the ξ-axis.

Equation (31) is the criterion that must be satisfied if the obliquity is to remain nearly constant. For Venus, P = 225 days, D = 243 days, $P_o \approx 8.10^4$ years. (This orbital precession period has been calculated using the secular disturbing functions for the earth and Jupiter. The period for each was calculated separately and the total period obtained by adding their contributions, i.e., $1/P_o = 1/P_\oplus + 1/P_{2\mathfrak{f}}$. This should afford a rough upper bound on the frequency of precession due to these planets.) Inserting these values the condition becomes

$$(C-A)/C >> 5 \times 10^{-6} |\sec\theta| \quad . \tag{38}$$

Using the equation for hydrostatic flattening, we obtain the lower limit $(C-A)/C_{min} \approx (k/3K) \times 6 \times 10^{-8}$. An Estimate of the J_2 term has been made by Anderson and Efron (1969) from the analysis of Mariner V tracking data. This implies an oblateness of $(C-A)/C = J_2/K = (1/K)(-5 \pm 10) \times 10^{-6}$. It appears that the ability of Venus to maintain a constant obliquity during precession of its orbit is marginal at best.

IV. TIDAL FRICTION AND GENERALIZED CASSINI'S LAWS

Up until now, we have dealt only with conservative forces. The study of these forces has enabled us to locate an axis, $\hat{\xi}$, for each object about which the spin axis describes a circular motion. There has not, however, been any light shed on the angular radius, θ, of this motion. The conservative forces, so far considered, furnish no constraints on this value. In this section, it shall be shown that it is the nonconservative tidal friction force which provides us with this information.

In 1693 Cassini stated his three famous laws governing the rotation of the moon (e.g., Danby, 1962):

(1) The moon rotates uniformly about its polar axis with a period equal to the mean sidereal period of its orbit about the earth.

(2) The inclination of the moon's equator to the ecliptic is a constant angle. (This angle is about $1^{\circ}35'$.)

(3) The ascending node of the lunar orbit on the ecliptic coincides with the descending node of the lunar equator on the ecliptic.

A little reflection reveals that laws (2) and (3) imply that the spin axis is coincident with $\hat{\xi}$, i.e., that the lunar spin axis executes circular motion about the ξ-axis with a vanishingly small radius, θ. In 1966 Colombo suggested that Mercury may be in a similar state. If the oblateness is large, $\hat{\xi}$ differs very little from $\hat{n}$ and the obliquity would be essentially zero. Colombo proposed that this configuration would be favored because it minimized internal friction. However, the time scale for energy dissipation by this process was unspecified and was admittedly questionable for objects with much longer precession periods than the moon. Peale (1969)

reopened the issue by introducing tidal interactions into the picture. It was first pointed out that the conditions $\theta = 0, \pi$ represents extremes in the body's pseudo-potential energy, E. This can be easily seen from equations (28) and (37). When $P_s \ll P_o$, E(0) is a minimum; when $P_s \gg P_o$, it is a maximum. For retrograde motion, $E(\pi)$ is always a minimum. Peale further contended that: "As E involves the energy of spin and orientation and angular momentum, any process which interchanges energy and angular momentum between the spin and orbital motions will drive E to an extreme value. Tidal interaction provides a mechanism of energy transfer which can either add or subtract energy associated with the spin and orientation." In this section, we shall put this contention on a firm computational footing utilizing a simple model of tidal torque orginally due to MacDonald (1964).

As a first step, the rate of energy change as a function of the tidal torque will be derived. Differentiating equation (19) with respect to time,*

$$dE/dt = -\alpha(\hat{s}\cdot\hat{n})(\hat{n}\cdot d\hat{s}/dt) - \Omega(\hat{k}\cdot d\hat{s}/dt). \tag{39}$$

Let $\bar{\chi}$ represent the time rate of change of $\hat{s}$ induced by the tidal torque, $\bar{\chi} = (d\hat{s}/dt)_T$. Adding this term to the left side of equation (13) furnishes the new equation of motion for $\hat{s}$,

$$d\hat{s}/dt = -\alpha(\hat{n}\cdot\hat{s})(\hat{n}\times\hat{s}) - \Omega(\hat{k}\times\hat{s}) + \bar{\chi} \quad . \tag{40}$$

Substituting equation (40) into (39) and employing well-known vector triple products yields the relation sought,

$$dE/dt = -\alpha(\hat{n}\cdot\hat{s})(\hat{n}\cdot\bar{\chi}) - \Omega(\hat{k}\cdot\bar{\chi}) \quad . \tag{41}$$

a) Frequency Dependent Q

The form of $\bar{\chi}$ must be obtained from the tidal torque. MacDonald calculates the torque by supposing that the equilibrium tidal bulge of the

*For simplicity, we assume $d\alpha/dt \approx 0$, which is nearly so during the terminal stage of despinning.

secondary is displaced from the subprimary point in the direction of the rotation by an angle, δ, given by the relation $\sin 2\delta = 1/Q$. Let $\hat{r}^*$ be a unit vector from the center of the secondary locating a point on the surface instantaneously at the subprimary point. Then this point, when viewed in a coordinate system rotating with the orbital angular velocity of the secondary, $\dot{v}$, moves according to the equation,

$$d\hat{r}^*/dt = (\bar{s} - \dot{v}\hat{n}) \times \hat{r}^*$$

where v is the true anomaly. If the orbit is circular, $\dot{v}$ is equal to the mean motion n. The direction of $d\hat{r}^*/dt$ gives the direction of the tidal bulge from the subprimary point. The torque exerted by the gravitational attraction of the primary for this bulge has the form $-(C/\tau)(\hat{r} \times d\hat{r}^*/dt)$, where C is the moment of inertia, τ, a characteristic time constant and $\hat{r}$, a fixed unit vector toward the primary. In the rotating system, the equation of motion for $\bar{s}$ is

$$\left.\frac{d\bar{s}}{dt}\right|_{rot} = -\frac{1}{\tau}\hat{r} \times [(\bar{s} - \bar{n}) \times \hat{r}^*] - (\bar{n} \times \bar{s}) \quad .$$

Transforming this equation to inertial space and using standard vector identities allows us to write,

$$\frac{d\bar{s}}{dt} = -\frac{1}{\tau}\left[(\bar{s} - \bar{n}) - \hat{r}(\hat{r} \cdot \bar{s})\right] \quad . \tag{42}$$

If $Q \propto (\text{frequency})^{-1}$, the characteristic time constant τ has the form

$$1/\tau \sim \frac{3k_T}{2Q_n} \cdot \frac{GM_p^2 R_s^5}{Cnr^6} \tag{43}$$

where k_T, R_s, and C are the tidal Love number, radius and moment of inertia of the secondary. Q_n is the value of Q for a frequency equal to n.

The orbital radius is denoted by r and M_p is the mass of the primary.

Since we are interested in time scales much longer than an orbit period, we can neglect these short-term variations by averaging equation (42) over an orbit,

$$\frac{d\bar{s}}{dt} = -\frac{1}{2\tau}\left\{\bar{s} + (\bar{s}\cdot\hat{n})\,\hat{n} - 2\bar{n}\right\} \quad . \tag{44}$$

We are interested in obtaining $(d\hat{s}/dt)_T = \bar{X}$,

$$\omega\left(\frac{d\hat{s}}{dt}\right)_T = \frac{d\bar{s}}{dt} - \hat{s}\frac{d\omega}{dt} \quad . \tag{45}$$

Dotting $\hat{s}$ into equation (44)

$$\frac{d\omega}{dt} = -\frac{1}{2\tau}\left\{\omega + \omega(\hat{s}\cdot\hat{n})^2 - 2(\hat{s}\cdot\hat{n})n\right\} \quad . \tag{46}$$

Substituting equations (44) and (46) into (45)

$$\left(\frac{ds}{dt}\right)_T = \bar{X} = \frac{1}{\tau}\left[\frac{n}{\omega} - \frac{1}{2}(\hat{s}\cdot\hat{n})\right]\left[\hat{n} - (\hat{s}\cdot\hat{n})\hat{s}\right] \quad . \tag{47}$$

This expression is to be used in equation (41) to evaluate dE/dt. Since the time scale for tidal decay is much longer than a precession period, we can average dE/dt over the latter. To obtain an answer accurate to second order in ξ and θ, we resolve $\hat{s}$ with respect to the coordinate system of figure 3,

$$\hat{s} = \cos\theta\,\hat{\xi} + \sin\theta\,[\cos\varphi\,\hat{x} + \sin\varphi\,\hat{y}]$$

and average over φ. A straight forward calculation yields,

$$\langle(\hat{k}\cdot\bar{\chi})\rangle \approx \frac{1}{\tau}\left(\frac{n}{\omega} - \tfrac{1}{2}\cos\xi\cos\theta\right)(\cos i - \cos\xi\cos(i-\xi)\cos^2\theta)$$

and

$$\langle(\hat{n}\cdot\hat{s})(\hat{n}\cdot\bar{\chi})\rangle \cong \frac{1}{\tau}\cos\xi\cos\theta\left(\frac{n}{\omega} - \tfrac{1}{2}\cos\xi\cos\theta\right)(1-\cos^2\xi\cos^2\theta) \quad .$$

Combining these to form $\langle dE/dt\rangle$

$$\langle dE/dt\rangle \cong -\frac{1}{\tau}\left(\frac{n}{\omega} - \tfrac{1}{2}\right)\Big\{(\alpha+\Omega\cos i)\sin^2\theta + (\alpha\cos\xi\sin^2\xi\cos\theta - \Omega\sin\xi\sin(i-\xi))\Big\} \quad .$$

However, the last two terms inside the second bracket cancel by virtue of equation (22), leaving

$$\langle dE/dt\rangle \approx -\frac{1}{\tau}\left(\frac{n}{\omega} - \tfrac{1}{2}\right)(\alpha + \Omega\cos i)\sin^2\theta \qquad (48)$$

In the terminal stage of tidal de-spinning as the secondary approaches synchronous rotation, the sign of the first bracket is positive. We note the following properties of $\langle dE/dt\rangle$: If $P_s \ll P_o$, α dominates and $\langle dE/dt\rangle < 0$. The quantity, E, approaches E (0) which is a minimum. When E = E(0), $\langle dE/dt\rangle$ vanishes. If $P_s \gg P_o$, Ω (which is negative) dominates and $\langle dE/dt\rangle > 0$. Again, we find E approaching E (0) which is now a maximum.

This demonstrates that for prograde motion, tidal friction drives the spin vector to coincidence with the ξ_o-axis, where $\xi_o = \xi(0)$. For retrograde motion, however, the spin axis does not approach the $\xi(\pi)$-axis. One can easily show that in that case, $\langle dE/dt \rangle$ is always positive. The pseudo-potential energy must consequently increase away from $E(\pi)$ which is a minimum. The retrograde spin of Venus is thus not stable in the presence of the solar tidal torque and other means must be found for maintaining the near 180° obliquity of this object (Goldreich and Peale, 1970).

b) Constant Q

If Q is assumed constant as has been suggested by MacDonald, then τ of equation (42) has the form,

$$1/\tau \sim \frac{3k_T}{2Q} \cdot \frac{GM_p^2 R_s^5}{Cr^6} \cdot |\hat{r}^* \times d\hat{r}^*/dt|^{-1} = \frac{\sigma}{|\hat{r}^* \times d\hat{r}^*/dt|} \qquad (49)$$

where from $d\hat{r}^*/dt$, we find

$$|\hat{r}^* \times d\hat{r}^*/dt|^2 = \omega^2 - 2\omega(\bar{n} \cdot \hat{s}) + n^2 - \omega^2 \sin^2 v[1 - (\hat{n} \cdot \hat{s})^2] . \qquad (50)$$

Note that this expression contains the true anomaly, v, which must be taken into account during orbital averaging of equation (42). If we define the following quantities,

$$C(\theta,\omega) = \frac{\omega}{2\pi} \int_0^{2\pi} \frac{\cos^2 v \, dv}{|\hat{r}^* \times d\hat{r}^*/dt|} \qquad (51)$$

$$S(\theta,\omega) = \frac{\omega}{2\pi} \int_0^{2\pi} \frac{\sin^2 v \, dv}{|\hat{r}^* \times d\hat{r}^*/dt|} \quad , \tag{52}$$

we can write this average as,

$$\frac{d\bar{s}}{dt} = -(\sigma/\omega)\left|C(\theta,\omega)\bar{s} + S(\theta,\omega)(\bar{s}\cdot\hat{n})\,\hat{n} - [C(\theta,\omega) + S(\theta,\omega)]\,\bar{n}\right| \quad . \tag{53}$$

Repeating the operations performed in (44) - (46),

$$d\omega/dt = -(\sigma/\omega)\{C(\theta,\omega)\,\omega + \omega S(\theta,\omega)(\hat{s}\cdot\hat{n})^2 - [C(\theta,\omega) + S(\theta,\omega)](\hat{s}\cdot\hat{n})n\}, \tag{54}$$

$$\left(\frac{ds}{dt}\right)_T = \bar{\chi} = -(\sigma/\omega)\,\{S(\theta,\omega)(\hat{s}\cdot\hat{n}) - \frac{n}{\omega}\,[C(\theta,\omega) + S(\theta,\omega)]\}[\hat{n} - (\hat{s}\cdot\hat{n})\,\hat{s}] \quad . \tag{55}$$

When this expression is substituted into equation (41) and averaged over an orbit one finds, as with the frequency dependent Q, that both $\langle\bar{\chi}\cdot\hat{k}\rangle$ and $\langle(\hat{s}\cdot\hat{n})(\bar{\chi}\cdot\hat{n})\rangle$ each have only one term that does not have $\sin^2\theta_o$ as a factor and these cancel when the expressions are combined to give $\langle dE/dt\rangle$,

$$\left\langle\frac{dE}{dt}\right\rangle \approx -(\sigma/\omega - n)\,\sin^2\theta\,(\alpha + \Omega\cos i)\left\{n/\omega - \tfrac{1}{2}\right\} \tag{56}$$

The remarks following (48) apply equally well to the above expression.

c) Physical Interpretation

The direction of $\bar{\chi}$ is given by $\hat{n} - \hat{s}(\hat{n}\cdot\hat{s})$ which is the component of $\hat{n}$ perpendicular to $\hat{s}$. It is clear that at any given instant, this torque is trying to rotate $\hat{s}$ into $\hat{n}$. We wish to inquire then, how such a torque could drive the spin vector coincident to the ξ-axis instead. The process is depicted schematically in Figure 4. This is a polar projection of the motion looking down the ξ-axis. In this example, $\hat{\xi}$ lies close to $\hat{n}$, $P_s \ll P_o$, and the

motion of the spin vector is nearly clockwise circular motion about $\hat{\xi}$. At a typical point such as O, the torque $\bar{\chi}$ is directed toward the tip of the orbit normal $\hat{n}$. The torque can be resolved into a component tangential to the path of $\hat{s}$ and a component directed toward the tip of $\hat{\xi}$. It is this latter, labeled $\bar{\chi}^*$, that is responsible for the decay of θ, the radius of the circular trajectory. The components of $\bar{\chi}^*$ to lowest order in ξ and θ are

$$\bar{\chi}^* = \chi^*(\omega)(\cos\xi \sin\theta_0 - \sin\xi \cos\theta_0 \sin\varphi)(\sin\theta_0 \hat{\xi} - \cos\theta_0 \hat{\varphi}) ,$$

where $\hat{\varphi}$ is a unit vector locating the angular position of O in the x,y plane. This expression vanishes at $\sin\varphi_c = \tan\theta_0 \cot\xi$ where $\bar{\chi}$ is completely tangential to the circle (points B and D). During the passage of $\hat{s}$ from B to D, the torque $\bar{\chi}^*$ tends to increase θ by pulling $\hat{s}$ toward $\hat{n}$. Its maximum effectiveness occurs at point C where $\bar{\chi}_c^* \propto \sin(\xi - \theta)[-\sin\theta_0 \hat{\xi} + \cos\theta_0 \hat{y}]$. However, from D back to B, the continued rotation $\hat{s}$ in the direction of $\hat{n}$ causes a corresponding decrease in θ. During this portion of the path, the torque achieves its greatest strength at point A, $\bar{\chi}_A^* \propto \sin(\xi + \theta_0)[\sin\theta \hat{\xi} + \cos\theta \hat{y}]$. Because the length of arc from D to B is longer and the torque is larger than from B to D, there is a small net decrease in the angle θ for each cycle of the precessional motion. We should also add, that had the assumption $d\alpha/dt \approx 0$ not been made, it would have been necessary to compute $dE(0)/dt$ also. We then would have been interested in the rate of change of $E - E(0)$. However, the conclusions are not altered by this modification.

Fig. 4. Decay of spin vector to $\hat{\xi}$. Circular path is spin vector trajectory. The time rate of change of the spin vector, $\bar{\chi}$, produced by tidal torque is always directed toward the orbit normal, $\hat{n}$. Over one cycle of the motion, the net effect of $\bar{\chi}$ is to decrease the radius, θ, of the cone of precession.

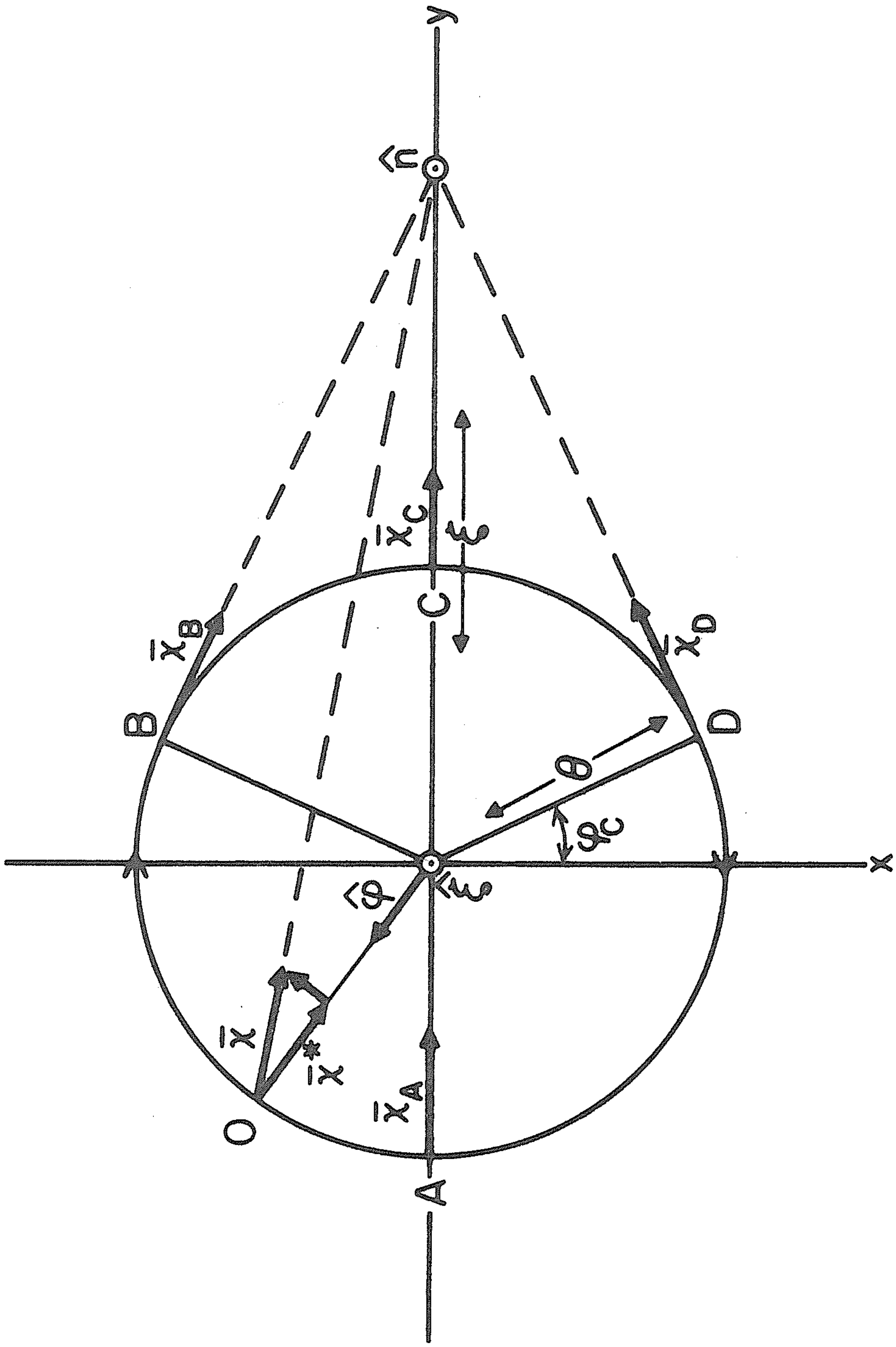
A
B
C
D
O
x
y

All of the objects considered in this paper have undergone severe tidal de-spinning and are presumably in their final rotation states. With the exceptions of Mercury and Venus, we can immediately conclude that the ξ_o-axis locations determined in Section III are quite likely also the positions of the spin axes of these bodies. Venus is excepted for the reason mentioned above. Mercury, on the otherhand, has had its "normal" process of tidal evolution interrupted. A detailed consideration of this planet will be the subject of the next section.

V. OBLIQUITY OF MERCURY

Radar measurements have determined the length of the Mercury day to be 58.7 days or 2/3 of the orbital period (Pettengill and Dyce, 1965; Dyce, Pettengill and Shapiro, 1967). The stability of this value in the presence of the solar tidal torque is presumed to be due to the influence of an additional torque arising from the attraction of the sun's mass for a permanent axial asymmetry of the planet (Colombo, 1965; Colombo and Shapiro, 1966; Goldreich and Peale, 1966). A net torque persists after averaging over an orbit because of the large eccentricity. As a consequence of the 2/3 commensurability, at successive perihelion passages the planet presents first one face and then the opposite to the sun. Because of this, the torque remains constant instead of averaging to zero over many orbits, as would be expected for a non-commensurable spin. The action of this torque is to spin up the planet by an amount that exactly compensates for the loss of angular momentum due to the solar tidal torque. Of course, this additional torque must also be included in the time evolution of the obliquity. The asymptotic spin rate predicted by tidal friction alone depends sensitively on the tidal model employed (Peale and Gold, 1965; Goldreich and Peale, 1966). However, there is reasonable accord between models as to the evolution of the spin vector up to the 3/2 resonance point. As an example, we shall first show that the frequency dependent model of tidal friction treated in this paper predicts a substantial obliquity for Mercury at the time it entered resonance. We shall then inquire as to whether the torque on the planet's intrinsic asymmetry could have a stabilizing influence on this obliquity analogous to its effect on the spin rate.

Because of the strong dependence of τ on r, the eccentricity must be taken into account when averaging the tidal torque (42) over an orbit. Writing $\tau = \tau_o(a/r)^6$, $r = a(1-e^2)/(1+e\cos v)$ and $\dot{v} = n(1+e\cos v)^2/(1-e^2)^{3/2}$, the average of a function f/τ takes the form

$$\langle f/\tau \rangle = \frac{1}{2\pi\tau_o}\int_o^{2\pi} dv\, \frac{(1-e\cos v)^4}{(1-e^2)^{3/2}}\, f$$

$$\approx \frac{1}{2\pi\tau_o}\int_o^{2\pi} dv f \left\{(1+\frac{9}{2}e^2) + 4e\cos v + 6e^2\cos^2 v\right\}$$

where we have retained terms to second order in e. The components of equation (42) for the tidal torque can be written,

$$\dot{S}_x = -(1/\tau)\left\{S_x \sin^2 v - S_y \sin v\cos v\right\} ,$$

$$\dot{S}_y = -(1/\tau)\left\{S_y \cos^2 v - S_x \sin v\cos v\right\} ,$$

$$\dot{S}_z = -(1/\tau)(S_z - n) .$$

When averaged over an orbit,

$$\langle \dot{S}_x \rangle = -(S_x/\tau_o)(\tfrac{1}{2}+3e^2) , \qquad (58a)$$

$$\langle \dot{S}_y \rangle = -(S_y/\tau_o)(\tfrac{1}{2}+9e^2/2) , \qquad (58b)$$

$$\langle \dot{S}_z \rangle = -(S_z/\tau_o)\{(1+13e^2/2) - (n/S_z)(1+27e^2/2)\} . \qquad (58c)$$

We have seen that the spin axis undergoes precession on a time scale of $\sim 2.4\cdot 10^3$ years [$(C-A)/C \sim 10^{-4}$]. Since this is short compared to the tidal time scale, we can average the above equations over this motion also. Multiplying equation (58a) by S_y and equation (58b) by S_x, adding these and averaging over a precession period yields,

$$\frac{d}{dt}(\omega \sin\theta) = -\frac{1}{\tau_o}\,\omega \sin\theta(\tfrac{1}{2}+15e^2/4) \ ,$$

where we have used $S_x = \omega \sin\theta \cos\varphi$ and $S_y = \omega \sin\theta \sin\varphi$. The angle, φ, measures the precession of the spin axis relative to the position of perihelion. The equation for $\langle \dot{S}_z \rangle$ remains unchanged and can easily be combined with the above to give

$$\frac{d\omega}{dt} = -\frac{\omega}{\tau_o}\left\{\tfrac{1}{2} + \cos\theta\left(\tfrac{1}{2}\cos\theta - \frac{n}{\omega}\right) + e^2\left[\left(\frac{11}{4}\cos\theta - \frac{27}{2}\frac{n}{\omega}\right)\cos\theta + \frac{15}{4}\right]\right\} \ , \tag{59}$$

$$\frac{d}{dt}\cos\theta = -\frac{\sin^2\theta}{\tau_o}\left\{\left(\tfrac{1}{2}\cos\theta - \frac{n}{\omega}\right) + e^2\left(\frac{11}{4}\cos\theta - \frac{27}{2}\frac{n}{\omega}\right)\right\} \ . \tag{60}$$

Note that as $t\to\infty$, $\theta\to o$; $\omega\to\omega_f$ where

$$\omega_f = n(1+27e^2/2)/(1+13e^2/2) \ .$$

Substitution of $e = 0.207$ produces $1.23n$ or a 71.5 day asymptotic rotation period for this model of tidal torque.

In Figure 5, we have integrated equations (59) and (60) with $e = 0.207$ for various values of the initial obliquity, θ_o. In all cases, the initial spin angular frequency was taken as $111n$. This value was deduced from MacDonald's (1964) relationship between spin angular momentum density and mass. We note that - although all curves converge on $(0, \omega_f)$ - at rotational rates slightly greater than the asymptotic value the obliquity is still rather large. In particular, at the 3/2 resonance most starting values for θ_o produce an obliquity near $\sim 34^\circ$. In all cases (except 90°) the obliquity at first rises steeply reaching a maximum where equation (60) equals zero, i.e.,

Fig. 5. Obliquity as a function of spin frequency for an object being despun by tidal friction. The asymptotic spin rate of 1.23n is a consequence of the MacDonald model employed. The 3/2 resonance position is marked. All evolutionary tracts considered have a sizable obliquity at this point.

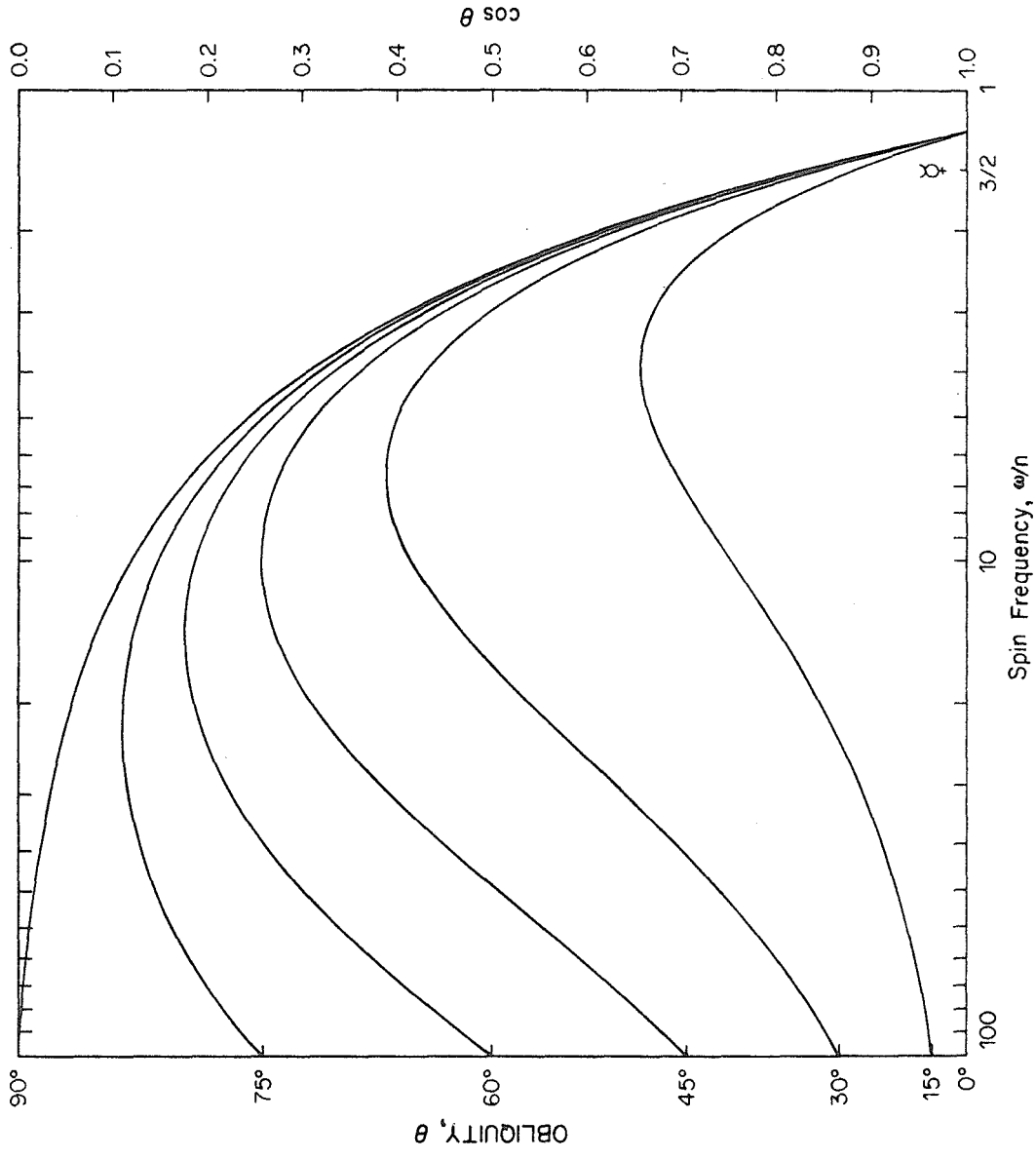
cos θ
0.0
0.1
0.2
0.3
0.4
0.5
0.6
0.7
0.8
0.9
1.0
1
3/2
10
100
Spin Frequency, ω/n
OBLIQUITY, θ
90°
75°
60°
45°
30°
15°
0°

$$\omega \cos\theta = 2n(1+27e^2/2)/(1+11e^2/2) \quad .$$

Actually, computations performed by Brouwer and Von Woerkom (1950) indicate that the eccentricity of Mercury varies between 0.11 and 0.24 with a period of about 2.2×10^5 years (Brouwer and Clemence, 1961b) so that e was not constant during the decay. Some idea of the sensitivity of the results on e can be found in Figure 6 where the equations were integrated for different values of e with $\theta_o = 20°$. This produced a rather regular variation of the resonance obliquity from 19° for e = 0.30 to 44° for e = 0.0.

If these results reasonably represent the de-spinning of a planet by tidal friction, then it appears likely that when Mercury achieved resonance it retained a sizable obliquity - perhaps larger than most observed in the solar system today. Further decay of the rotational frequency stopped. We now address ourselves to the evolution of the obliquity in this resonance state.

The gravitational torque exerted by a primary on a secondary with three unequal moments of inertia can be written;

$$\bar{T} = \frac{3\mu}{r^3} \left\{ (C-B)(\hat{r}\cdot\hat{J})(\hat{r}\cdot\hat{K})\,\hat{I} + (A-C)(\hat{r}\cdot\hat{K})(\hat{r}\cdot\hat{I})\,\hat{J} + (B-A)(\hat{r}\cdot\hat{J})(\hat{r}\cdot\hat{I})\,\hat{K} \right\} \qquad (61)$$

where μ is the product of the primary's mass and the gravitational constant, $A < B < C$ are the three principal moments of inertia of the secondary, $\hat{I}$, $\hat{J}$, and $\hat{K}$ are unit vectors along the principal axes of its inertial ellipsoid, $\hat{r}$ is a unit vector locating the primary from the center of the secondary, and r, the separation of the bodies. Suppose a planet is spinning in the 3/2 resonance state with zero obliquity. The planet alternately presents one face and then the opposite to the sun at perihelion. If at a given passage the

Fig. 6. Obliquity as function of spin frequency during tidal friction despinning for different values of the orbital eccentricity. For the MacDonald model of tidal friction used, the asymptotic spin rate is a function of the eccentricity.

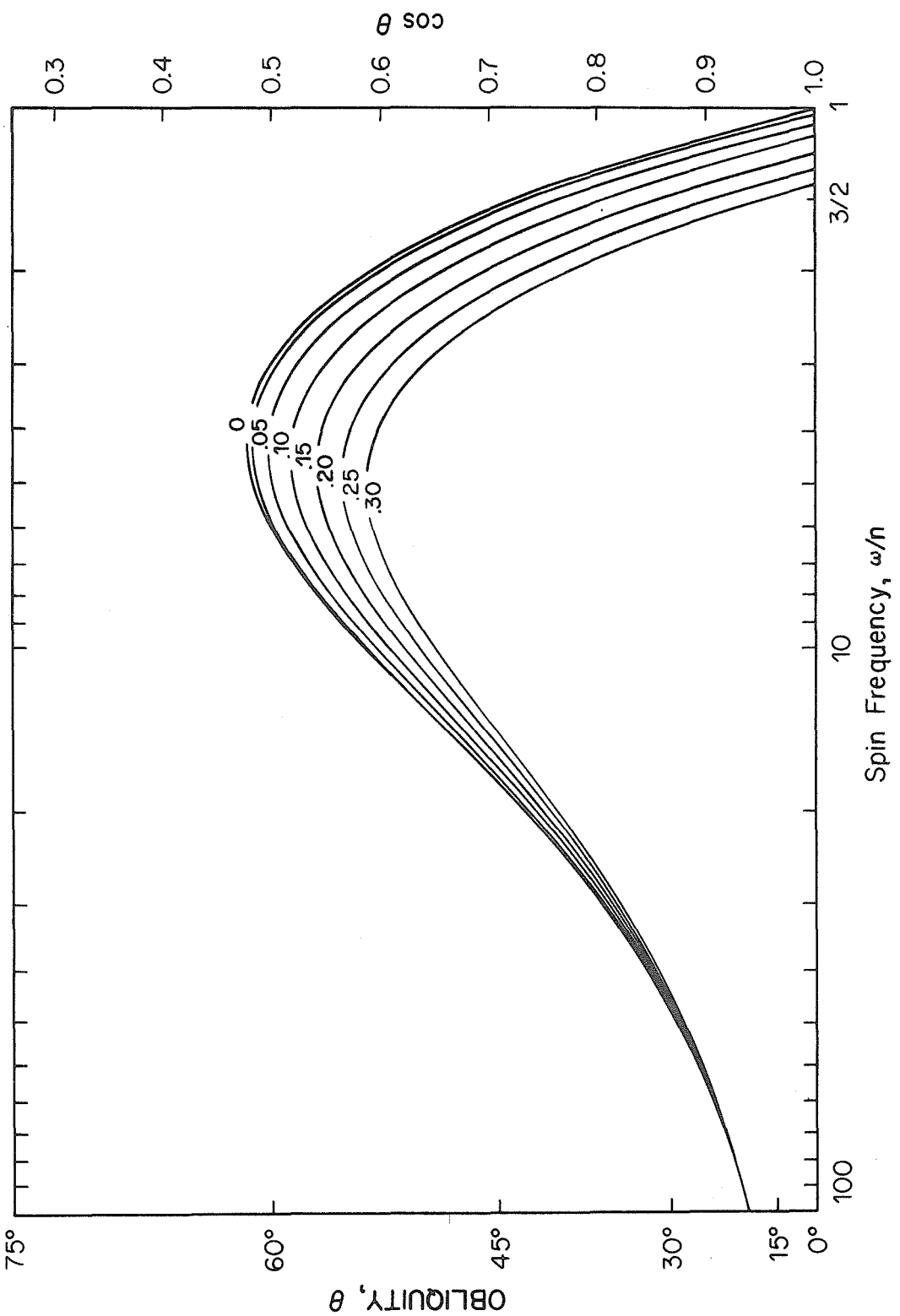
OBLIQUITY, θ
75°
60°
45°
30°
15°
0°
cos θ
0.3
0.4
0.5
0.6
0.7
0.8
0.9
1.0
0
.05
.10
.15
.20
.25
.30
100
10
3/2
1
Spin Frequency, ω/n

axis of the minimum moment of inertia, A, makes an angle α with the solar direction, $\hat{r}$, then the angle remains constant at each subsequent passage as long as the resonance is maintained. Let us now define an inertial coordinate system with unit vectors $\hat{x}$, $\hat{y}$, $\hat{z}$ which coincide with the principal axes at perihelion of the hypothetical planet just described. This system is pictured in Figure 7. Now consider a planet with a spin axis which instead of being in the $\hat{z}$ direction is located by the angles (θ, φ) in the inertial system. The azimuthal angle, φ, changes as the planet undergoes precession. When the planet is at perihelion, its principal axes can be located by tipping $\hat{z}$ into $\hat{s}$ in such a way that the coordinate system suffers no rotation about its z axis, i.e., the coordinate system is transformed by rotating it about an axis $\hat{\theta} = (\hat{s}\times\hat{z})/|\hat{s}\times\hat{z}|$. The principal axes at perihelion, denoted by primes, are related to the original set of unit vectors by,

$$\hat{I}' = (\cos\theta\cos^2\varphi + \sin^2\varphi)\,\hat{x} - (1-\cos\theta)\cos\varphi\sin\varphi\,\hat{y} - \cos\varphi\sin\theta\,\hat{z}\ ,$$

$$\hat{J}' = -(1-\cos\theta)\sin\varphi\cos\varphi\,\hat{x} + (\cos\theta\sin^2\varphi + \cos^2\varphi)\,\hat{y} - \sin\varphi\sin\theta\,\hat{z}\ ,$$

$$\hat{K}' = \hat{s} = \sin\theta\cos\varphi\,\hat{x} + \sin\theta\sin\varphi\,\hat{y} + \cos\theta\,\hat{z}\ .$$

Since the planet is spinning with an angular velocity $\omega = (3/2)n$, the principal axes as a function of time measured from the moment of perihelion passage are

$$\hat{I} = \hat{I}'\cos\omega t + \hat{J}'\sin\omega t\ ,$$

$$\hat{J} = -\hat{I}'\sin\omega t + \hat{J}'\cos\omega t\ ,$$

$$\hat{K} = \hat{K}'\ .$$

In addition, $\hat{r}$ and r are functions of the orbital position of the planet,

$$\hat{r} = \cos(\alpha + v)\,\hat{x} + \sin(\alpha + v)\,\hat{y}\ ,$$

$$r = a(1 - e^2)/(1 + e\cos v)\ .$$

Fig. 7. Principal axes at perihelion for an object in the 3/2 resonance state and with an obliquity, $\theta > 0$.

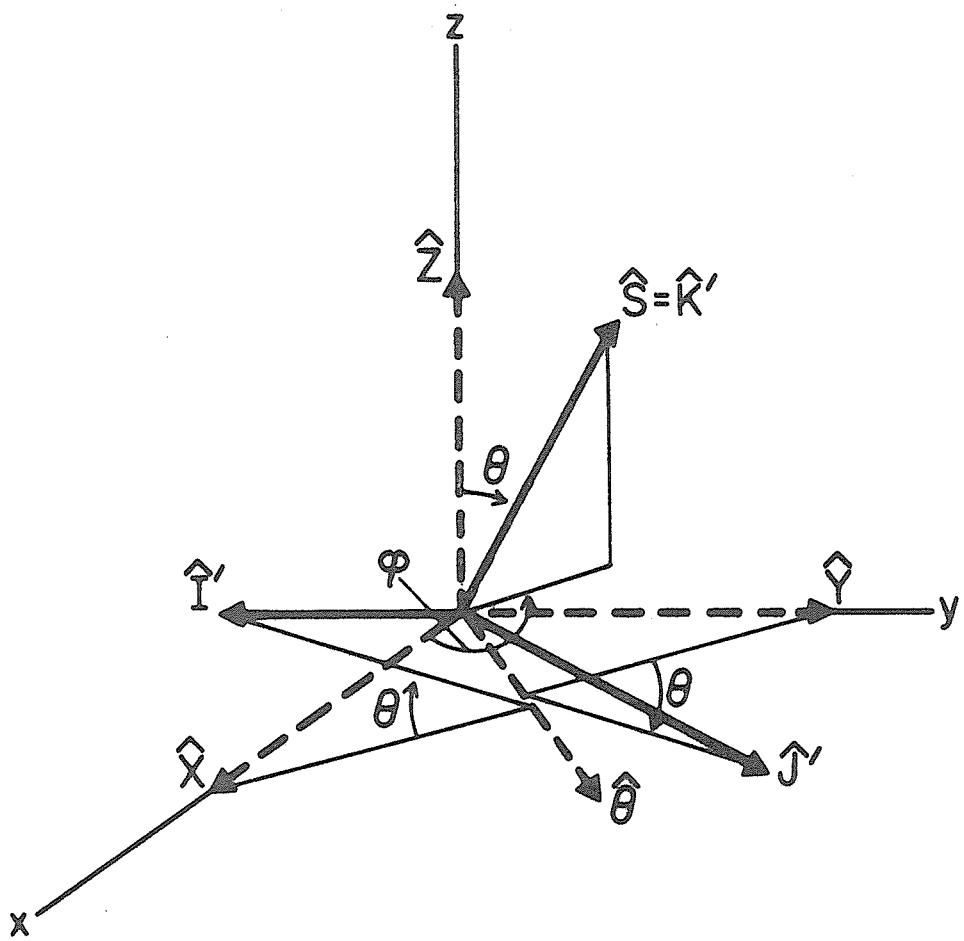
z
$\hat{Z}$
$\hat{S}=\hat{K}'$
θ
$\hat{I}'$
φ
$\hat{Y}$
y
θ
θ
$\hat{X}$
$\hat{J}'$
$\hat{\theta}$
x

Internal dissipation constrains the planet to rotate about its maximum principal moment of inertia C. In the absence of other torques, the equation of motion for the rotational angular velocity is $C\,d\bar{s}/dt = \bar{T}$. Taking the dot product of this equation with $\hat{K}'$ gives the time rate of change of ω,

$$C\frac{d\omega}{dt} = \hat{K}'\cdot\bar{T}$$

while the dot product with $\hat{z}$ gives the time rate of change of $S_z = \omega\cos\theta$,

$$C\frac{dS_z}{dt} = \hat{z}\cdot\bar{T} \quad .$$

Both of these equations are to be averaged over orbital and precessional periods,

$$\langle f\rangle = \frac{1}{2\pi}\int_0^{2\pi} d\varphi\cdot\left\{\frac{1}{2\pi a^2(1-e^2)^{\frac{1}{2}}}\int_0^{2\pi} dv\; r^2 f(v,\varphi)\right\} \quad .$$

It is advantageous at this point to interchange the order of integration,

$$\langle f\rangle = \frac{1}{4\pi^2 a^2(1-e^2)^{\frac{1}{2}}}\int_0^{2\pi} dv\left\{r^2\int_0^{2\pi} d\varphi\; f(v,\varphi)\right\} \quad .$$

Averaging over the precession angle is straightforward but lengthy. The results are as follows, (Appendix),

$$\langle\hat{K}\cdot\bar{T}\rangle_\varphi = \frac{3\mu}{8r^3}(B-A)(1+\cos\theta)^2\sin 2(v+\alpha-\omega t) \quad , \tag{62}$$

$$\langle\hat{z}\cdot\bar{T}\rangle_\varphi = \frac{-3\mu}{8r^3}(C-B)\sin^2\theta\,(1+\cos\theta)\sin 2(v+\alpha-\omega t)$$

$$-\frac{3\mu}{8r^3}(A-C)\sin^2\theta\,(1+\cos\theta)\sin 2(v+\alpha-\omega t)$$

$$+\frac{3\mu}{8r^3}(B-A)\cos\theta\,(1+\cos\theta)^2\sin 2(v+\alpha-\omega t)$$

$$= \frac{3\mu}{8r^3}(B-A)(1+\cos\theta)^2 \sin 2(v+\alpha-\omega t) \quad . \tag{63}$$

Note that $\langle \hat{K} \cdot \bar{T} \rangle_{\varphi} = \langle \hat{z} \cdot \bar{T} \rangle_{\varphi}$. We now must average these values over an orbit,

$$\frac{3n^2}{8}(B-A)(1+\cos\theta)^2 \frac{1}{2\pi}\int_0^{2\pi} dv \frac{(1+e\cos v)}{(1-e^2)^{3/2}} \sin 2(v+\alpha-\omega t) \quad . \tag{64}$$

We shall obtain a solution to first order in e. We can express ωt in terms of v from the conservation of angular momentum. To first order, $nt \approx v - 2e \sin v$. Since $\omega = (3/2)n$, the integrand of equation (64) becomes

$$\sin(2\alpha - v) + e\cos v \sin(2\alpha - v) + 6e \sin v \cos(2\alpha - v) \quad .$$

Integrating over a cycle while holding α constant yields $7\pi e \sin 2\alpha$. The twice averaged expressions for the time rates of change of ω and $\omega\cos\theta$ are

$$\left\langle \frac{d\omega}{dt} \right\rangle = \left\langle \frac{d}{dt}\omega\cos\theta \right\rangle = \frac{21}{16} en^2 \left(\frac{B-A}{C}\right)(1+\cos\theta)^2 \sin 2\alpha \quad . \tag{65}$$

Since these rates are equal, it is apparent that they cannot both act to cancel out their (unequal) tidal counterparts. Clearly, if the resonance state is to survive, then we must have,

$$\left\langle \frac{d\omega}{dt} \right\rangle_T + \left\langle \frac{d\omega}{dt} \right\rangle_P = 0 \quad , \tag{66}$$

where the subscripts T and P denote tidal and permanent asymmetry torques. The total rate of change of the obliquity can now be obtained from

$$\frac{d}{dt}\cos\theta = \frac{1}{\omega}\left\langle \frac{dS_z}{dt} \right\rangle_T + \frac{1}{\omega}\left\langle \frac{dS_z}{dt} \right\rangle_P \quad . \tag{67}$$

Using equations (65) and (66) to eliminate the second term leads to the expression

Fig. 8. Decay of the obliquity of an object locked into the 3/2 resonance spin state as a function of the characteristic tidal decay time, τ_o.

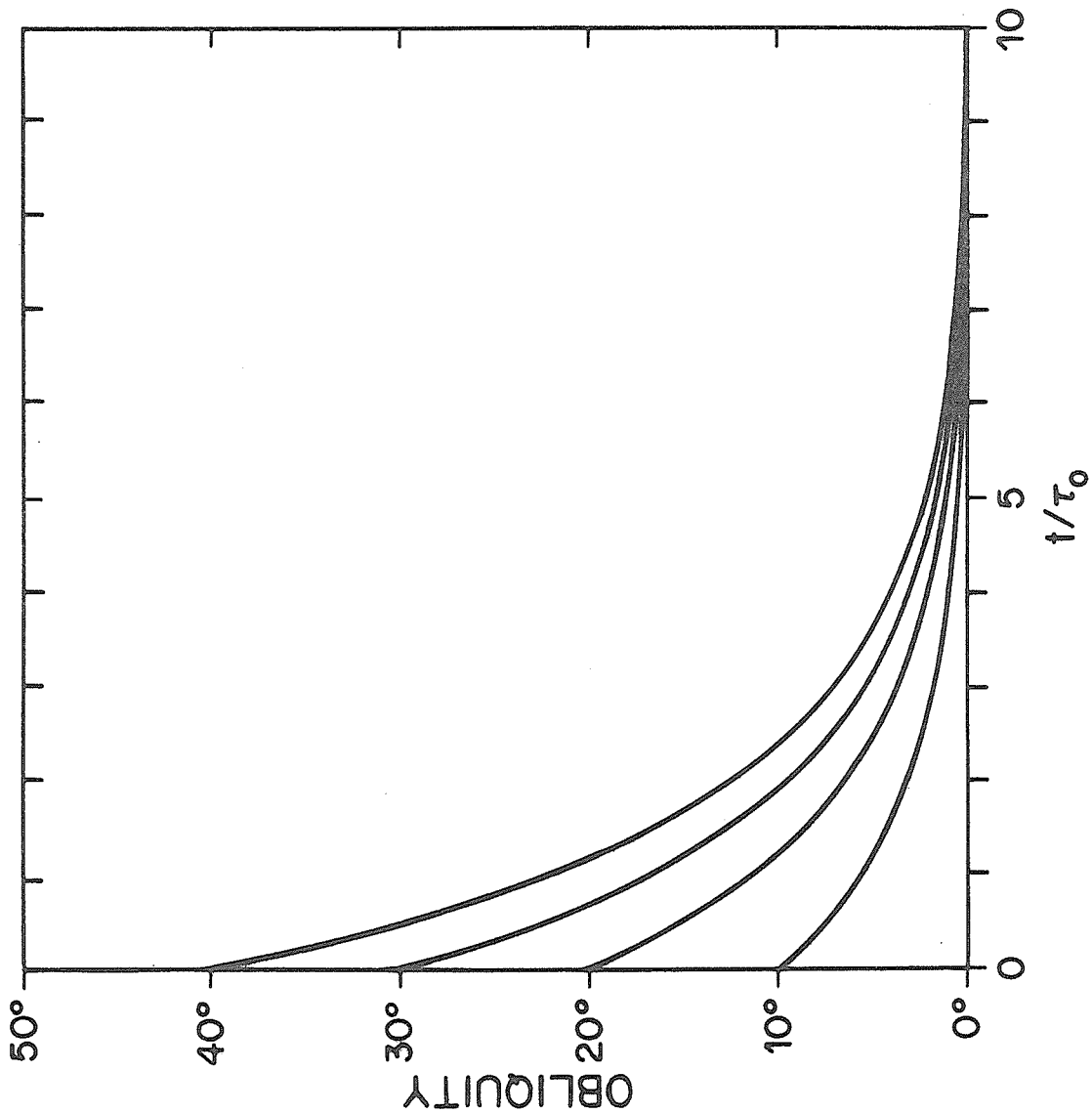
OBLIQUITY
50°
40°
30°
20°
10°
0°
0
5
10
t/τ₀

$$\frac{d}{dt}\cos\theta = \frac{1}{\tau_o}(1-\cos\theta)\left\{\frac{1}{6}(7-3\cos\theta) + \frac{e^2}{4}(51-11\cos\theta)\right\}. \quad (68)$$

This expression is positive for all values of θ so that the obliquity always decays. Integrating (68) with $a = 7/6 + 51e^2/4$ and $b = \frac{1}{8} + 11e^2/4$,

$$\cos\theta = (1 - ac)/(1 - bc)$$

$$c = \left(\frac{1-\cos\theta'}{a-b\cos\theta'}\right)\exp\left\{-(a-b)\,t/\tau_o\right\}. \quad (69)$$

This expression is plotted in Figure 8 for several values of θ', the obliquity at the beginning of resonance. The decay rate is essentially the same as that for non-resonance. This is because there are two largely compensating changes resulting from resonance. First, since the decay of ω stops, $\cos\theta = S_z/\omega$ no longer receives a corresponding positive increment. On the other hand, dS_z/dt switches from a negative value for non-resonance to a positive one for resonance reestablishing the decay rate. Estimating $k_T \sim 0.1$ and $K \sim 0.4$, yields a value of 2×10^5 Q_n years for the characteristic tidal decay time.

We conclude from the inability of the asymmetry torque to stabilize the obliquity, that - as with most other tidally de-spun objects in the solar system - the rotation axis of Mercury has been driven parallel to its ξ_o-axis which, for likely values of $(C-A)/C$, implies an essentially zero obliquity for this planet. At this time, the best determination of the orientation of the spin axis appears to be by optical observations. According to Peale (1972), B.A. Smith has put an upper limit at $\sim 3^\circ$.

VI. OBLIQUITY OF VENUS

It has been pointed out (Goldreich and Peale, 1970) that the present action of the solar tidal torque on Venus is to decrease the obliquity, i.e., turn the planet upright. It was suggested by these authors that the present near 180° obliquity of Venus is maintained by a dominant opposing torque. Assuming that Venus has a core similar to the earth's, the requisite torque owes its existence to differential motion at the core-mantle boundary. The precession of the mantle due to the attraction of the sun for the planet's figure is communicated to the core via viscous coupling with an attendant energy dissipation which damps the component of the spin vector lying in the orbit plane. Because the core lags behind the mantle, the spin axes of these two units are not coincident. The external torque producing the precession is perpendicular to the spin axis of the mantle but has a component antiparallel to the total angular momentum. It is this component which counteracts the solar tidal torque. The spin vector is driven perpendicular to the orbit plane thus suppressing the precession. However, from the results of the present paper, it is clear that the obliquity cannot be 180° unless the position of the orbit normal changes in inertial space on a time scale long compared to the energy dissipation time, i.e., a few times a spin precession period.

The equations of motion for the core and mantle taken by Goldreich and Peale were the following:

$$C_m \frac{d\bar{s}_m}{dt} = -\frac{3}{2}\frac{GM_\odot}{a^3}(C_m - A_m)(\hat{n}\cdot\hat{s}_m)(\hat{n}\times\hat{s}_m) - \lambda(\bar{s}_m - \bar{s}_c) , \tag{70}$$

$$C_c \frac{d\bar{s}_c}{dt} = \lambda(\bar{s}_m - \bar{s}_c) . \tag{71}$$

The angular velocities and moments of inertia for the mantle and core are designated by the appropriate subscripts. The torque on the figure of the planet is assumed to act only on the mantle. The torque on the core due to viscous coupling is set proportional to the vector difference of the core and mantle spins. The coupling constant λ is to be related to the physical properties of the core.

These equations yield an exponential decay of the obliquity with a time constant given by

$$\tau = \frac{C_m}{\lambda}\left\{1 + \left[\frac{\lambda}{\dot{\varphi}}\left(\frac{1}{C_m} + \frac{1}{C_c}\right)\right]^2\right\} , \tag{72}$$

where $\dot{\varphi}$ is the precession frequency of the mantle. For $C_c/C_m = 0.1$, the minimum value of τ is 3.5 precession periods when $(\lambda/\dot{\varphi})(1/C_m + 1/C_c) = 1$. If the motion is retrograde, this decay will oppose and dominate the effect of the solar tidal torque for obliquities greater than some critical value (see Goldreich and Peale, 1970).

To equations (70) and (71), we add another for the precession of the orbit plane,

$$\frac{d\hat{n}}{dt} = -\Omega(\hat{n}\times\hat{k})$$

with the solution given by expression (8). For simplicity let us assume $\hat{n}$ revolves about $\hat{k}$ quickly compared to the precession of $\hat{s}_m$ and $\hat{s}_c$. Substituting for $\hat{n}$ in equation (70) and averaging over the short time scale yields

$$C_m \frac{d\bar{s}_m}{dt} = -\frac{3}{2}\frac{GM_\odot}{a^3}(C_m - A_m)(\hat{n}\cdot\hat{k})(\hat{k}\cdot\hat{s}_m)(\hat{k}\times\hat{s}_m) - \lambda(\bar{s}_m - \bar{s}_c) . \tag{73}$$

With this equation in place of (70) the solution preceeds exactly as before

with one important difference: Instead of driving the spin axis antiparallel to the orbit normal, $\hat{n}$, it decays antiparallel to the normal of the invariable plane, $\hat{k}$.

In general, the spin vector approaches $-\hat{\xi}$. For more comparable values of P_s and P_o as suggested by Anderson's determination of the J_2 term, this axis lies somewhere between $\hat{n}$ and $\hat{k}$. Our best guess at present, is that core-mantle coupling of the type proposed by Goldreich and Peale will produce a final obliquity between one and two degrees short of 180°.

Radar determinations of the spin vector orientation are tenuous at best. However the results to date tend to support a few degrees deviation from 180°. Shapiro (1967) reports a value of ~178.5° while Carpenter (1970) finds an obliquity of ~174°.

VII CONCLUSION

We considered three processes in the solar system by which the orbit plane of a secondary can be induced to execute precession: (1) gravitational perturbations by a second orbiting object, (2) the torque exerted by an oblate primary, and (3) the locking of the orbit plane to the equator plane of a precessing primary. In addition, the spin axis of an oblate secondary precesses as a result of the torque arising from the gravitational attraction of the primary. When examined in conjunction with the orbit precession, the spin axis is found to undergo nearly uniform precession about an auxiliary vector, $\hat{\xi}$, which remains always coplanar with the orbit normal, $\hat{n}$, and the normal to the invariable plane, $\hat{k}$, about which $\hat{n}$ rotates. The angular separation between $\hat{\xi}$ and the orbit normal is determined by the ratio of the spin precession period to the period for orbit precession, P_s/P_o. If $P_s/P_o \ll 1$, $\hat{\xi}$ is nearly coincident with the orbit normal and the obliquity of the secondary remains very nearly constant throughout the motion. This is the situation for the equatorial satellites of Mars, Jupiter, Saturn, and Uranus (case (3)). This is also very nearly true for Mercury (case (1)) provided $(C - A)/C$ is on the order of 10^{-4} as might be anticipated from our knowledge of the lunar oblateness. Even if Triton has an oblateness determined only by hydrostatic flattening, the spin axis of this object (case (2)) can follow its orbit normal rather well. On the other hand, the small J_2 term measured by Mariner V indicates that the spin axis of Venus (case (1)) is relatively unable to follow its orbit normal and that the ξ-axis is inclined to the orbit normal by one or two degrees.

All of the objects treated in this paper have been strongly de-spun by tidal friction. We have shown that tidal friction also drives the spin axis in the direction

of $\hat{\xi}$. The time scale for this process is comparable to that necessary to achieve sychronous rotation. Even in the case of Mercury where a sychronous rotation has not been established, it was found that the 3/2 resonance state did not significantly alter this process. Hence, we believe that these objects exhibit a generalization of Cassini's laws where the spin axis, orbit normal, and normal to the invariable plane, remain always coplanar. Venus is an exception since its retrograde spin axis is surely not in the direction of $\hat{\xi}$. However, if the retrograde rotation is maintained by friction at a core-mantle boundary, the spin axis should be driven antiparallel to $\hat{\xi}$ and a Cassini type motion should still prevail. Hence, we expect the obliquity of Venus to be one or two degrees short of 180°.

APPENDIX

Average of Permanent Asymmetry Torque Over a Cycle of Spin Axis Precession

The equation for the time rate of change of the spin frequency is $C d\omega/dt = \hat{K} \cdot \bar{T}$. From equation (61),

$$\hat{K} \cdot \bar{T} = \frac{3\mu}{r^3} (B-A)(\hat{r} \cdot \hat{J})(\hat{r} \cdot \hat{I}) \quad . \tag{A1}$$

This expression is to be averaged over a cycle in φ. Using the expression relating $\hat{I}$, $\hat{J}$, and $\hat{r}$ to the inertial space unit vectors $\hat{x}$, $\hat{y}$, $\hat{z}$ one finds,

$$\begin{aligned}(\hat{r} \cdot \hat{J})(\hat{r} \cdot \hat{I}) = \{&-(\hat{I}' \cdot \hat{x}) \sin\omega t \cos(\alpha+v) - (\hat{I}' \cdot \hat{y}) \sin\omega t \sin(\alpha+v) \\ &+ (\hat{J}' \cdot \hat{x}) \cos\omega t \cos(\alpha+v) + (\hat{J}' \cdot \hat{y}) \cos\omega t \sin(\alpha+v)\} \\ &\cdot \{(\hat{I}' \cdot \hat{x}) \cdot \cos\omega t \cos(\alpha+v) + (\hat{I}' \cdot \hat{y}) \cos\omega t \sin(\alpha+v) \\ &+ (\hat{J}' \cdot \hat{x}) \sin\omega t \cos(\alpha+v) + (\hat{J}' \cdot \hat{y}) \sin\omega t \sin(\alpha+v)\} \quad . \end{aligned} \tag{A2}$$

where

$$\begin{aligned}(\hat{I}' \cdot \hat{x}) &= \cos\theta \cos^2\varphi + \sin^2\varphi \\ (\hat{I}' \cdot \hat{y}) &= (\hat{J}' \cdot \hat{x}) = -(1-\cos\theta) \sin\varphi \cos\varphi \\ (\hat{J}' \cdot \hat{y}) &= \cos\theta \sin^2\varphi + \cos^2\varphi \quad . \end{aligned} \tag{A3}$$

Multiplying out (B2) leads to various combinations of (B3) which are then to be averaged over φ. Upon doing so we find,

$$\begin{aligned}&\langle(\hat{I}' \cdot \hat{x})^2\rangle = \langle(\hat{J}' \cdot \hat{y})^2\rangle = \frac{3}{8}\cos^2\theta + \frac{1}{4}\cos\theta + \frac{3}{8} \quad , \\ &\langle(\hat{I}' \cdot \hat{x})(\hat{J}' \cdot \hat{y})\rangle = \frac{1}{8}\{\cos^2\theta + 6\cos\theta + 1\} \quad , \\ &\langle(\hat{J}' \cdot \hat{x})^2\rangle = \langle(\hat{I}' \cdot \hat{y})^2\rangle = \langle(\hat{J}' \cdot \hat{x})(\hat{I}' \cdot \hat{y})\rangle = \frac{1}{8}(1-\cos\theta)^2 \quad , \\ &\langle(\hat{I}' \cdot \hat{x})(\hat{J}' \cdot \hat{x})\rangle = \langle(\hat{I}' \cdot \hat{y})(\hat{J}' \cdot \hat{y})\rangle = \langle(\hat{I}' \cdot \hat{x})(\hat{I}' \cdot \hat{y})\rangle \\ &\qquad = \langle(\hat{J}' \cdot \hat{x})(\hat{J}' \cdot \hat{y})\rangle = 0 \quad . \end{aligned} \tag{A4}$$

The surviving part of (B2) can be written,

$$\cos^2(\alpha+v)\,\sin\omega t\,\cos\omega t\left\{\frac{1}{8}(1-\cos\theta)^2 - \frac{3}{8}\cos^2\theta - \frac{1}{4}\cos\theta - \frac{3}{8}\right\}$$

$$- \sin^2(\alpha+v)\,\sin\omega t\,\cos\omega t\left\{\frac{1}{8}(1-\cos\theta)^2 - \frac{3}{8}\cos^2\theta - \frac{1}{4}\cos\theta - \frac{3}{8}\right\}$$

$$- \cos(\alpha+v)\,\sin(\alpha+v)\,\sin^2\omega t\left\{\frac{1}{8}(\cos^2\theta+6\cos\theta+1) + \frac{1}{8}(1-\cos\theta)^2\right\}$$

$$+ \cos(\alpha+v)\sin(\alpha+v)\,\cos^2\omega t\left\{\frac{1}{8}(\cos^2\theta+6\cos\theta+1) + \frac{1}{8}(1-\cos\theta)^2\right\} \qquad \text{(A5)}$$

$$= -\frac{1}{8}\cos 2(\alpha+v)\,\sin 2\omega t\,(1+\cos\theta)^2$$

$$+ \frac{1}{8}\sin 2(\alpha+v)\,\cos 2\omega t\,(1+\cos\theta)^2$$

$$= \frac{1}{8}(1+\cos\theta)^2\,\sin 2(\alpha+v-\omega t) \quad .$$

Hence,

$$\langle \hat{K}\cdot\bar{T}\rangle_{\varphi} = \frac{3\mu}{8r^3}(B-A)(1+\cos\theta)^2\,\sin 2(\alpha+v-\omega t) \quad . \qquad \text{(A6)}$$

The equation for the time rate of change of $S_z = \omega\cos\theta$ is $C\,dS_z/dt = \hat{z}\cdot\bar{T}$. From equation (61),

$$\hat{z}\cdot\bar{T} = \frac{3\mu}{r^3}\Big\{(C-B)(\hat{r}\cdot\hat{J})(\hat{r}\cdot\hat{K})(\hat{z}\cdot\hat{I}) + (A-C)(\hat{r}\cdot\hat{K})(\hat{r}\cdot\hat{I})(\hat{z}\cdot\hat{J})$$

$$+ (B-A)(\hat{r}\cdot\hat{J})(\hat{r}\cdot\hat{I})(\hat{z}\cdot\hat{K})\Big\} \quad . \qquad \text{(A7)}$$

The last term is simply $\cos\theta\,(\hat{K}\cdot\bar{T})$ so that its contribution can be obtained from (B6). In addition to the expressions, (B3), we require,

$$(\hat{z}\cdot\hat{I}') = -\cos\Psi\,\sin\theta \quad , \quad (\hat{z}\cdot\hat{J}') = -\sin\Psi\,\sin\theta \quad , \qquad \text{(A8)}$$

$$(\hat{k}\cdot\hat{x}) = \sin\theta\,\cos\varphi \quad , \quad (\hat{K}\cdot\hat{y}) = \sin\theta\sin\varphi \quad .$$

Next we write out the product $(\hat{r}\cdot\hat{J})(\hat{r}\cdot\hat{K})(\hat{z}\cdot\hat{I})$,

$$(\hat{r}\cdot\hat{J})(\hat{r}\cdot\hat{K})(\hat{z}\cdot\hat{I}) = \Big\{-(\hat{I}'\cdot\hat{x})\sin\omega t\cos(\alpha+v) - (\hat{I}'\cdot\hat{y})\sin\omega t\sin(\alpha+v)$$
$$+ (\hat{J}'\cdot\hat{x})\cos\omega t\cos(\alpha+v) + (\hat{J}'\cdot\hat{y})\cos\omega t\sin(\alpha+v)\Big\}$$
$$\cdot\Big\{(\hat{K}'\cdot\hat{x})\cos(\alpha+v) + (\hat{K}'\cdot\hat{y})\sin(\alpha+v)\Big\}$$
$$\cdot\Big\{(\hat{z}\cdot\hat{I}')\cos\omega t + (\hat{z}\cdot\hat{J}')\sin\omega t\Big\} \quad . \qquad (A9)$$

The various combinations of the three dot products when averaged produce the following results;

$$\langle(\hat{K}'\cdot\hat{x})(\hat{z}\cdot\hat{I}')(\hat{I}'\cdot\hat{x})\rangle = \langle(\hat{K}'\cdot\hat{y})(\hat{z}\cdot\hat{J}')(\hat{J}'\cdot\hat{y})\rangle$$
$$= -\sin^2\theta\left\{\frac{3}{8}\cos\theta + \frac{1}{8}\right\} \quad ,$$
$$\langle(\hat{K}'\cdot\hat{x})(\hat{z}\cdot\hat{I}')(\hat{J}'\cdot\hat{y})\rangle = \langle(\hat{K}'\cdot\hat{y})(\hat{z}\cdot\hat{J}')(\hat{I}'\cdot\hat{x})\rangle$$
$$= -\sin^2\theta\left\{\frac{1}{8}\cos\theta + \frac{3}{8}\right\} \quad ,$$
$$\langle(\hat{K}'\cdot\hat{x})(\hat{z}\cdot\hat{J}')(\hat{I}'\cdot\hat{y})\rangle = \langle(\hat{K}'\cdot\hat{x})(\hat{z}\cdot\hat{J}')(\hat{J}'\cdot\hat{x})\rangle =$$
$$\langle(\hat{K}'\cdot\hat{y})(\hat{z}\cdot\hat{I}')(\hat{I}'\cdot\hat{y})\rangle = \langle(\hat{K}'\cdot\hat{y})(\hat{z}\cdot\hat{I}')(\hat{J}'\cdot\hat{x})\rangle =$$
$$\frac{1}{8}\sin^2\theta\,(1-\cos\theta) \quad .$$

All other combinations yield zero upon averaging over φ. The surviving part of $(\hat{r}\cdot\hat{J})(\hat{r}\cdot\hat{K})(\hat{z}\cdot\hat{I})$ is,

$$\frac{1}{2}\cos^2(\alpha+v)\sin 2\omega t\left\{\frac{1}{8}\sin^2\theta(1-\cos\theta) + \sin^2\theta\left(\frac{3}{8}\cos\theta + \frac{1}{8}\right)\right\}$$
$$+\frac{1}{2}\sin^2(\alpha+v)\sin 2\omega t\left\{-\frac{1}{8}\sin^2\theta(1-\cos\theta) - \sin^2\theta\left(\frac{3}{8}\cos\theta + \frac{1}{8}\right)\right\}$$
$$+\frac{1}{2}\cos^2\omega t\sin 2(\alpha+v)\left\{-\sin^2\theta\left(\frac{1}{8}\cos\theta+\frac{3}{8}\right) + \frac{1}{8}\sin^2\theta\,(1-\cos\theta)\right\}$$
$$+\frac{1}{2}\sin^2\omega t\sin 2(\alpha+v)\left\{\sin^2\theta\left(\frac{1}{8}\cos\theta+\frac{3}{8}\right) - \frac{1}{8}\sin^2\theta\,(1-\cos\theta)\right\}$$

$$= \frac{1}{2} \cos 2(\alpha+v) \sin 2\omega t \left\{ \frac{1}{8} \sin^2\theta \ (1-\cos\theta) + \sin^2\theta \left(\frac{3}{8} \cos\theta + \frac{1}{8} \right) \right\}$$

$$- \frac{1}{2} \sin 2(\alpha+v) \cos 2\omega t \left\{ \sin^2\theta \left(\frac{1}{8} \cos\theta + \frac{3}{8} \right) - \frac{1}{8} \sin^2\theta \ (1-\cos\theta) \right\}$$

$$= -\frac{1}{8} \sin 2(\alpha+v-\omega t) \sin^2\theta \ (1+\cos\theta) \ .$$

Hence, we find the first term of equation (B7) contributes,

$$-\frac{3}{8} \frac{\mu}{r^3} (C-B) \sin^2\theta \ (1+\cos\theta) \sin 2(\alpha+v-\omega t) \ .$$

By a similar procedure, one can show that the second term contributes,

$$-\frac{3}{8} \frac{\mu}{r^3} (A-C) \sin^2\theta \ (1+\cos\theta) \sin 2(\alpha+v-\omega t) \ .$$

REFERENCES

Allen, C. W., 1963, Astrophysical Quantities, Second Edition, Athlone Press, London.

Anderson, J.D., and Efron, L., 1969, "Mass and Dynamical Oblatness of Venus", (A), Bull. Amer. Astron. Soc., 1, 231.

Anderson, J. D., Efron, L., and Pease, G. E., 1968, "Mass, Dynamical Oblateness, and Position of Venus as Determined by Mariner V Tracking Data", Astron. J., 73, S162 (Abstract).

Brouwer, D. and Von Woerkom, A.J.J., 1950, "The Secular Variations of the Orbital Elements of the Principal Planets", Astr. Papers Amer. Ephem. Naut. Almanac, Vol. 13, Part 2.

Brouwer, D. and Clemence, G. M., 1961a, Methods of Celestial Mechanics, Academic Press, New York.

Brouwer, D. and Clemence, G. M., 1961b, in Planets and Satellites, Kuiper, G. P., ed., University of Chicago Press.

Carpenter, R. L., 1964, "Study of Venus by CW Radar", Astron. J., 69, 2-11.

Carpenter, R. L., 1970, "A Radar Determination of the Rotation of Venus", Astron. J., 75, 61-66.

Cassini, G. D., 1693, Traite de L'origine ede Progress de L'Astronomie, Paris.

Colombo, G., 1965, "Rotational Period of the Planet Mercury", Nature, 208, 575.

Colombo, G., 1966, "Cassini's Second and Third Laws", Astron. J., 71, 891-896.

Colombo, G. and Shapiro, I. I., 1966, "Rotation of the Planet Mercury", Ap. J., 145, 296-307.

Danby, J. M. A., 1962, Fundamentals of Celestial Mechanics, The Macmillan Company, New York.

Dyce, R. B., Pettengill, G. H., and Shapiro, I. I., 1967, "Radar Determination of the Rotations of Venus and Mercury", Astron. J., 72, 351-359.

Goldreich, P., 1965, "Inclination of Satellite Orbits about an Oblate Precessing Planet", Astron. J., 70, 5-9.

Goldreich, P. and Peale, S. J., 1966, "Spin-Orbit Coupling in the Solar System", Astron. J., 71, 425-438.

Goldreich, P. and Toomre, A., 1969, "Some Remarks on Polar Wandering", J.G.R., 2555-2567.

Goldreich, P. and Peale, S. J., 1970, "Obliquity of Venus", Astron. J., 75, 273-284.

Goldstein, H., 1950, Classical Mechanics, Addison-Wesley Publishing Co., Reading, Massachusetts.

Jet Propulsion Laboratory Report No. 32-1306, 1971.

Lewis, J. S., 1971, "Satellites of the Outer Planets: Their Physical and Chemical Nature", Icarus, 15, 174-185.

Lorell, J., Born, G. H., Christensen, E. J., Jordon, J. F., Laing, P. A., Martin, W. L., Sjorgren, W. L., Shapiro, I. I., Reasenberg, R. D., and Slater, G. L., 1972, "Mariner IX Celestial Mechanics Experiment: Gravity Field and Pole Direction of Mars", Science, 175.

MacDonald, G. J. F., 1964, "Tidal Friction", Rev. Geophys., 2, 464-541.

Munk, W. H. and MacDonald, G. J. F., 1960, The Rotation of the Earth, Cambridge University Press, New York.

Peale, S. J. and Gold, T., 1965, "Rotation of the Planet Mercury", Nature, 206, 1241.

Peale, S. J., 1969, "Generalized Cassini's Laws", Astron. J., 74, 483-489.

Peale, S. J., 1972, "Determination of Parameters Related to the Interior of Mercury", Icarus, 17, 168-173.

Pettengill, G.H., Dyce, R.B., 1965, "A Radar Determination of the Rotation of the Planet Mercury", Nature, 206, 1240.

Shapiro, I. I., 1967, "Resonance Rotation of Venus", Science, 157, 423.

Tisserand, F., 1896, Traite de Celeste, Vol. 4, Gauthier-Villars, Paris.

Widorn, T., 1950, Sitz. Oster. Akad. Wiss., Wien, Ser. IIa, 159.